Supporting Information

for

Xenobiotics Targeting Cardiolipin Metabolism to Promote Thrombosis in Zebrafish

Hang Liu, Hongyang Cui, Yixuan Huang, Shixiong Gao, Shu Tao, Jianying Hu, Yi Wan*

[1]*Laboratory for Earth Surface Processes,* College of Urban and Environmental Sciences, Peking University, Beijing 100871, China

*Address for Correspondence:

Dr. Yi WAN,

College of Urban and Environmental Sciences,

Peking University,

Beijing 100871, China,

TEL & FAX: 86-10-62759126,

Email: wany@urban.pku.edu.cn.

Text

Table

Figure

Figure S1. A workflow diagram of this study.

Figure S2. PCA analysis of screened metabolites during the developing stages of zebrafish embryos (6 to 120 h post fertilization), and concentration changes of representative molecules of the screened metabolites.

Figure S3. Selected molecules obtained by network analysis and OPLSDA.

Figure S4. Distributions of exposure chemicals and their metabolites detected in the auto-generated network.

Figure S5-S24. Mass spectra of identified metabolites and corresponding standards detected in zebrafish embryo.

Figure S25. Dose-response of LPCs, LPEs, linoleate related PUFAs, PLs, CL and Sep in zebrafish embryos after exposures to pp′-DDE, TPHP, PFOS, and TCS.

Figure S26-S27. Metabolic pathways between CLs and linoleate related PUFAs validated by stable isotope tracing.

Figure S28-S30. Metabolic pathways between CLs and linoleate related PUFAs validated by rescue experiments.

Figure S31. Levels of TAZ in zebrafish embryos exposed to the 11 chemicals.

Figure S32. Variations in CL levels in zebrafish embryos exposed to TCS or co-exposed to TCS and ISO.

Figure S33. Levels of ACAs, PGI_2, and TXA_2 in zebrafish embryos exposed to the CL disrupting chemicals (pp′-DDE, TPHP, PFOS, and TCS) and CL at different concentrations.

Figure S34. O-dianisidine staining of heart RBCs and the RBC intensities in zebrafish embryos exposed to pp′-DDE, TPHP, PFOS and PHZ at different concentrations. Heart rates and

histopathological examination of thrombus in blood vessels of zebrafish embryo exposed to PHZ.

Maintenance of Zebrafish.

AB strain wild-type zebrafish (4–5 months old) were maintained in purified aquaculture water (pH of 7.2 ± 0.2) at 27 ± 1°C with a photoperiod of 14/10 (light/dark), and were fed twice daily with live brine shrimp (*Artemia nauplii*). Adult male and female zebrafish were paired at a ratio 2:1 in a breeding tank overnight and separated with a mesh screen before spawning. Spawning and fertilization started within 30 min after removal of the screen. Embryos were collected at 2 hours post-fertilization (hpf) and rinsed twice with purified aquaculture water. Normally developed embryos were screened under a stereomicroscope (M165FC, Leica) and collected for exposure experiments.

Sample Preparations.

First, 800 μL of iced methanol was added to the collected embryos, which were then homogenized in the lysing matrix tubes at a speed of 6.0 m/s for 30 s. The sample mixtures were, then divided into two equal portions and transferred into 4-mL vials for separate extraction of polar (fraction 1, F1) and non-polar (fraction 2, F2) components. F1 was fully deproteinized with 1.1 mL of ice-cold methanol. To F2, 100 μL of ultrapure water was added and vortexed for 2 min to precipitate proteins before the addition of 1.4 mL of ice-cold MTBE. All F1 and F2 fractions were sonicated at 4°C for 30 min and then centrifuged for 20 min (4°C, 7,500 rpm). The supernatants of F1 and F2 were collected and then lyophilized to dryness. The residues were re-dissolved in 200 μL of methanol/water (1:1, v:v) (F1) or chloroform/methanol/water (1:2:0.8, v:v:v) (F2), and filtered through a hydrophobic PTFE filter (13 mm, 0.22 μm) for Ultraperformance Liquid Chromatography Quadrupole Time-of-flight Mass Spectrometry (UPLC-QTOF-MS) analysis. The extraction processes have been

validated by analysis of embryos spiked with ^{13}C-labeled Lauric acid, D7-SPH, 16:0-D31 SM, 16:0 D31-18:1 PI, 16:0 D31-18:1 PC, and 16:0 D31-18:1 PG, and the recoveries were in the range of 73-102% and 65-91% for polar and non-polar fractions, respectively.

Screening by High Resolution Mass Spectrometry.

A UPLC-QTOF-MS system (Xevo G2, Waters) operating in both the positive (ESI^+) and negative (ESI^-) electrospray ionization modes was used to obtain the full mass spectra of the metabolites in the zebrafish embryos. Chromatographic separation was performed on 5-μL samples via an ACQUITY UPLC BEH C8 column (2.1 mm × 50 mm, 1.7 μm particle size) at 40°C: solvent A was 10 mM ammonium acetate in ultrapure water, solvent B was acetonitrile, and the flow rate was 0.3 mL/min. The chromatographic elution programs in both the positive and negative modes were as follows: 30% B was initially held for 0.5 min, and the eluent was then ramped to 80% B by 3.5 min and 100% B by 6.0 min, and then held for 0.5 min, before being returned to the initial conditions by 6.5 min and equilibrated for 1.5 min before injection of the next sample. The UPLC-QTOF-MS was operated at a resolution of 25,000 and 1 s scan time. The high-accuracy MS^E data were acquired in continuum mode with an m/z range of 50–1,600 for the precursor ions and corresponding fragments. In low energy mode, data were collected with a constant collision energy of 3 V, and in elevated energy mode, the collision energy was ramped from 15 to 55 V. The other optimized MS parameters were as follows: source capillary voltage, 3 kV (ESI^+) or 2 kV (ESI^-); sampling cone voltage, 30 V (ESI^+) or 45 V (ESI^-); extraction cone voltage, 4 V; source temperature, 150°C; desolvation temperature, 350°C (ESI^+) or 450°C (ESI^-); cone gas flow, 50 L/h; and desolvation gas flow, 600 L/h (ESI^+) or 800 L/h (ESI^-).

The UHPLC-Orbitrap MS (Q-Exactive system, Thermo Fischer Scientific) was further used to confirm and/or identify the screened metabolites in embryos. In the mode of full scan MS/data-dependent (dd) MS^2, the full scan resolution was set at 70,000, and the ddMS^2 resolution was set at 17,500. The adjusted parameters for electrospray ionization mode were set as follows: spray voltages of 3.5 kV and 2.8 kV were used for positive and negative modes, respectively; the capillary temperature was maintained at 325°C; and the sheath gas flow and auxiliary gas flow were set to 40 Arb and 10 Arb, respectively. The S-lens RF level was 50.

Visualized Networking of Mass Signals.

A visualized network of all screened mass signals was automatically generated through correlation network analysis.[1] A correlation matrix was constructed through analysis of unique signal-signal pairs on the basis of all mass signals detected in samples from different exposed groups. The correlated pairs were selected with absolute values of the Pearson correlation coefficient (R) higher than 0.7[2] and further processed in Gephi 0.9.2 (Gephi Consortium, France) to generate the correlation network. Each discrete molecule was represented as a node, and the corresponding pairwise connections were represented as links between two paired compounds in the network. The layout algorithms of OpenOrd and Force Atlas were used to automatically generate the core clusters of the compounds. The sizes of nodes were set according to the signal abundances for embryos from the control group. The nodes were shaded in different colors showing the degrees of signal intensity: warm colors from yellow to purple represented a gradual increase in intensity, and cool colors from blue to green represented a corresponding decrease.

Identifications of Mass Signals.

Preliminary analysis of embryos was used to determine the general ionizations of metabolites molecules in zebrafish embryos. The adduct ion forms in ESI^+ mode were selected as $[M+H]^+$, $[M+NH4]^+$, $[M+Na]^+$, $[M+K]^+$, $[M+H-H_2O]^+$, $[M+H-2H_2O]^+$, $[M+CH_3OH+H]^+$, $[M+ACN+H]^+$, $[M+ACN+Na]^+$, $[2M+H]^+$, $[2M+Na]^+$, $[M+2H]^{2+}$, and $[M+2H-2H_2O]^{2+}$; and those in ESI^- mode were $[M-H]^-$, $[M-H2O-H]^-$, $[M+FA-H]^-$, $[M+CH_3COO]^-$, $[M+Cl]^-$, $[2M-H]^-$, $[M-2H]^{2-}$, $[M+Na-2H]^{2-}$, and $[M+K-2H]^{2-}$. In peak identification, mass signals were identified by software-based searching the following databases: the Human Metabolome Database (HMDB), Kyoto Encyclopedia of Genes and Genomes (KEGG), Lipid Maps, Mass Bank, PubChem, and PubMed.[1] The remaining unmatched mass signals were then identified by searching the National Institute of Standards and Technology (NIST), BioCyc, Cayman chemical, Small Molecule Pathway Database (SMPDB), and the Manchester Centre for Integrative Systems Biology (MCISB) databases.[3-5] The mass tolerances for precursors and corresponding fragment ions were set to 10 ppm.

The identified and unknown signals were further confirmed and/or identified with UHPLC-Orbitrap HRMS with higher resolutions and sensitivities. The raw data obtained from the UHPLC-Q-Exactive™ were processed in Compound Discoverer 2.1 software (Thermo Fisher, Waltham, MA). Mass signals were identified by software-based searching the corresponding database mzCloud.[6] The mass tolerance was set to 5 ppm, and peaks with MS/MS spectra containing at least two product ions matched with the database were selected. The final identification results retained the peaks with higher abundances and matching rates.

The auto-generated network enhanced the confidence of metabolite identifications, since signals that belonged to the same cluster generally have close metabolic relationships. The

optimal identification was achieved under the guidance of signals with high identification levels in each cluster. The duplicate identified results were manually screened in ESI^+ and ESI^- modes for both F1 and F2 fractions.

Validation of Identified Metabolites.

All metabolites were identified on the basis of the MS and corresponding fragmentation information recorded in online databases, which were classified as a second level of identification.[7] A network was generated, and the metabolites were divided into several clusters. Approximately 77 major metabolites from each core cluster with important metabolic significance or high detection frequency were selected for further validation. The corresponding 77 commercial standards with the same or similar structures were purchased. The MS and fragmentation patterns generated by collision-induced dissociations in the MS^E analysis were compared between samples and standards to achieve first-level identification of the crucial metabolites.

Quantification of Chemicals in Exposed Embryos.

Concentrations of chemicals were determined in the exposed embryos. The protocols of sample preparations for determining chemical concentrations were based on previous studies.[8-12] After 96 h exposure, embryos were collected and rinsed with deionized water for three times. The embryos were transferred into 2 mL pre-weighed glass bottles, weighted after removing excess water, and stored at -80 ℃ until analysis. 10 embryos were homogenized as one sample in 400 μL deionized water, and four replicate samples were analyzed per treatment. The polled samples were added with surrogate standards and underwent liquid-liquid extraction for gas chromatography coupled with mass spectrometry (GC-MS) or UPLC-MS/MS analysis.

Phenolic compounds including BPA, 6OHBDE47, and TCS were quantified relative to ^{13}C-BPA; TPHP and TPT were quantified relative to TPHP-d_{15}; PCB153 and pp′-DDE were quantified relative to PCB121; B(a)P was quantified relative to perylene-d_{14}; and PFOS, PFOA, and DEHP were quantified relative to ^{13}C-PFOS, ^{13}C-PFOA, and DEHP-d_4, respectively.

Pooled embryo samples used for analysis of BPA, 6OHBDE47, TCS, TPT, PCB153, pp′-DDE, and B(a)P were extracted with 1 mL hexane four times. The aquatic fraction was then passed through sodium sulfate to remove any moisture and eluted with 1 mL of hexane and 1 mL of dichloromethane. The extracts were dried and re-dissolved in 100 μL hexane for GC-MS analysis of PCB153, pp′-DDE, and B(a)P, or re-dissolved in 100 μL methanol for UPLC-MS/MS analysis of BPA, 6OHBDE47, TCS, and TPT.

Pooled samples used for quantification of PFOS and PFOA were added with 1 mL TBAS and 2 mL Na_2CO_3, and then extracted with 5 mL MTBE. Supernatant extracts were transferred after vigorously shaking at 3000 rpm for 15 min, sonicating for 15 min, and centrifuging at 3500 rpm for 15 min. Samples used for quantification of DEHP were firstly added with 800 μL acetonitrile and then extracted with 1 mL hexane. Supernatant extracts were transferred after sonicating for 20 min, and centrifuging at 2500 × g for 5 min. Samples used for quantification of TPHP were extracted with 3 mL acetonitrile. Supernatant extracts were transferred after centrifuging at 400 rpm for 10 min. The extraction of PFOS, PFOA, DEHP, and TPHP repeated three times, and the extracts were dried and concentrated to 100 μL (methanol) for UPLC-MS/MS analysis. Recovery experiments were conducted to checked the analytical procedures, and recovery rates of target compounds were in the range of 78.6-100.4% in zebrafish embryos.

PCB153, pp′-DDE, and B(a)P were determined by a GC-MS (6890/5973, Agilent) equipped with a fused silica capillary column (DB-5MS, 30 m × 250 μm, 0.25 μm). The injector was maintained at 250 ℃ at a splitless mode. The column oven temperature was programmed to increase from 70 ℃ to 220 ℃ (held 3 min) at the rate of 20 ℃/min, to 300 ℃ (held 5 min) at the rate of 20 ℃/min. The interface temperature and ion source were held at 280 ℃ and 250 ℃, respectively. The carrier gas was helium at a constant flow rate of 2 mL/min.

A UPLC-MS/MS system (Xevo TQ-XS, Waters) operating in both the positive (ESI^+) and negative (ESI^-) electrospray ionization modes was used to determine the concentrations of BPA, 6OHBDE47, TCS, TPT, PFOS, PFOA, DEHP, and TPHP according to previous studies.[10-13] DEHP, TPHP, and TPT were determined in positive mode and BPA, 6OHBDE47, TCS, PFOS, and PFOA were analyzed in negative mode. Chromatographic separation was conducted using an ACQUITY UPLC BEH C8 column (2.1 mm × 50 mm, 1.7 μm particle size) at 40°C, and the flow rate and injection volume were 0.3 mL/min and 5 μL, respectively. 5 mM ammonium acetate in ultrapure water (A) and acetonitrile (B) were used as mobile phases. 25% B was initially held for 0.5 min, and the eluent was then ramped to 95% by 6.0 min, and then held for 2 min, before being returned to the initial condition by 8.1 min and equilibrated for 1.9 min before injection of the next sample. The optimum conditions in the ESI source were: source temperature, 150 ℃； desolvation temperature, 500 ℃; capillary voltage, 3.00 kV (ESI^+) or 1.00 kV (ESI^-); desolvation gas flow, 1000 L/h (ESI^+) or 600 L/h (ESI^-); and cone gas flow 150 L/h. Quantitative analysis of the target chemicals was performed in multi-selected reaction monitoring (MRM), and the dwell time were automatically selected at 20 ms (ESI^+) and 60 ms (ESI^-). The optimized MRM conditions of target chemicals were provided in Table S3.

Stable Isotope Tracing.

^{13}C-labeled linoleate was used to track the pathways between linoleate related PUFAs and CLs. Zebrafish embryos were co-exposed to pp′-DDE and linoleate or ^{13}C-labeled linoleate according to the exposure conditions listed above. The exposure concentrations of pp′-DDE and linoleate/^{13}C-linoleate were 100 and 1000 ng/mL, respectively. Samples from the groups exposed to linoleate and ^{13}C-linoleate were screened with UHPLC-Orbitrap HRMS, and the differences in signals from the two groups were compared. Only the signals with differences of 1.0034 (MW difference between ^{13}C-labeled Lin and Lin) from the two groups were selected and identified. The identified ^{13}C-labeled metabolites provided pathway information allowing us to link the metabolism of linoleate to that of CLs.

Rescue Experiments.

Rescue experiments were conducted for further validation of the associations between linoleate related PUFAs and CLs. Four chemicals including pp′-DDE, TPHP, PFOS, and TCS were found to elevate the levels of CLs and to decrease the levels of linoleate/arachidonate/α-linoleate. Thus, pp′-DDE and TCS were selected and used for zebrafish embryo co-exposure with linoleate/arachidonate/α-linoleate separately. Levels of CLs in embryos were determined and compared between the pp′-DDE/TCS single exposure group and pp′-DDE/TCS+linoleate/arachidonate/α-linoleate co-exposed groups. The associations between linoleate related metabolites and CLs could be theoretically validated if the addition of linoleate/arachidonate/α-linoleate significantly inhibited the increase in CLs induced by exposure to selected chemicals. The exposure concentrations of pp′-DDE, TCS, and linoleate/arachidonate/α-linoleate were 100 ng/mL, 50 ng/mL, and 1000 ng/mL, respectively.

The same method was also used to verify the relationship between ISO and CLs. TCS was selected because it is the only chemical that simultaneously induced a decrease in ISO and an increase in CLs. The exposure concentrations of ISO and TCS were 2000 and 50 ng/mL, respectively. The relationship between ISO and CLs could be theoretically validated if the addition of ISO significantly inhibited the increase in CLs induced by TCS.

Enzyme-linked Immunosorbent Assay (ELISA) Tests.

The catalysis of the metabolic reactions is governed by the enzymes of the regulatory network, and ELISA has been widely used to assess the activities of enzymes in the metabolic conversion of lipids.[14-18] In this study, the enzymes including LPLAT, LCLAT, PLA_2, CLS, TAZ, and XOD, which catalyzes the synthesis and/or metabolism of PLs, LPLs, and CLs, have been validated based on the reported studies.[19-22] The levels of ACA antibodies including IgA, IgG, and IgM, and prostaglandins (PGI_2 and TXA_2) associated with thrombosis were generally measured by a standardized ELISA.[23-25] The analyses were conducted with kits designed for zebrafish. The embryos exposed to the 11 target chemicals were collected for the ELISA tests, and the embryos exposed to CL (18:1 CL) at different concentrations were also subjected to the ELISA tests. A total of 100 exposed embryos were uniformly collected per sample. ELISA tests were conducted according to the instructions provided by the kits. The materials in the kits were shown in Table S4. All reagents were prepared before starting the assay procedure. About 50 μL of standard was added to the standard well. 10 μL of testing sample was added to the sample wells and then added with 40 μl sample diluent. No reagents were added to the blank wells. 100 μL of HRP-conjugate reagent were then added to each well, covered with an adhesive strip, and incubated for 60 min at 37 °C. After incubation, each well was aspirated, and rinsed with wash

solution (400 μL), which were repeated for four times. After the last wash, remaining wash solutions were completely removed in each well. 50 μL chromogen solution A and 50 μL chromogen solution B were added to each well, and gently mixed and incubated for 15 min at 37°C. 50 μL stop solution was finally added to the well, and the optical density at 450 nm were determined with a microplate reader (Multiskan FC, Thermo Scientific) within 15 min.

Assessment of Thrombotic Symptoms.

Determining the amount of heart red blood cells (RBCs) has been demonstrated to be a promising method for quantification of thrombosis.[26,27] pp′-DDE, TPHP, PFOS, and TCS were selected because of their potential to elevate the levels of CLs. Embryos were exposed to three levels (low, medium, and high) of each chemical, as described above. Embryos were also exposed to 18:1 CL at concentrations of 100 ng/mL, 500 ng/mL, and 2000 ng/mL. After exposure, all zebrafish were stained with O-dianisidine to quantify the heart RBCs in zebrafish.[26,27] A total of 25 zebrafish from each group were randomly chosen to be immobilized in 3% methyl cellulose. The heart RBC images were acquired in the identical lighting intensity at 80× magnification under a dissecting stereomicroscope (SZX7, OLYMPUS, Japan) with a high-speed video camera (VertA1, China). NIS-Elements D3.10 image analysis software (Nikon) was subsequently used to estimate the average RBCs intensity for erythrocyte positive staining in the cardiac region. To confirm that PHZ-induced thrombus formation in the caudal vein was accompanied by a reduction of heart RBCs intensity, we performed histopathological examination after treatment. Zebrafish were first fixed in 4% paraformaldehyde (in 0.1 M phosphate-buffered saline) for 4 h at 4°C, and then dehydrated in graded series of ethanol solutions. Embedded zebrafish were longitudinally

sectioned at 5 μm and stained with hematoxylin and eosin to acquire histological images at a 400× magnification under a histological microscope (Leica, Germany). Because tachycardia is another critical thrombotic symptom, the heart rate was measured in 96-hpf exposed embryos randomly selected from each group. The heart rates were counted and recorded under a stereomicroscope (M165FC, Leica).

297 **Table S1.** Chemicals, enzyme-linked immunosorbent assay kits, software, and standards of
298 metabolites used for method optimization, metabolite identification, rescue experiments, and
299 isotope tracing.

REAGENT or RESOURCE	SOURCE	IDENTIFIER
Exposure chemicals		
Bisphenol A (BPA)	Sigma-Aldrich	Cat#239658
Benzo(a)pyrene (B(a)P)	Sigma-Aldrich	Cat#51968
Bis(2-ethylhexyl) phthalate (DEHP)	Sigma-Aldrich	Cat#36735
1,1-bis-(4-chlorophenyl)-2,2-dichloroethene (pp′-DDE)	Sigma-Aldrich	Cat#35487
Perfluorooctanoate (PFOA)	Dr. Ehrenstorfer GmbH	Cat#C15987150
Perfluorooctane sulfonate (PFOS)	Dr. Ehrenstorfer GmbH	Cat#C15987120
2,2′,4,4′,5,5′-hexachlorobiphenyl (PCB153)	Dr. Ehrenstorfer GmbH	Cat#C20015300
Triphenyl phosphate (TPHP)	Dr. Ehrenstorfer GmbH	Cat#C17893000
6-hydroxy-2,2′,4,4′-tetrabromodiphenyl ether (6OHBDE47)	AccuStandard	Cat#HBDE-4005S-CN-0.2X
Triphenyltin chloride (TPT)	AccuStandard	Cat#P-526N
Triclosan (TCS)	Wellington Laboratories	Cat#3380-34-5
Internal/Surrogate standards		
Bisphenol A-^{13}C (^{13}C-BPA)	Santa Cruz	Cat#sc-217773
Triphenyl-d_{15} phosphate (TPHP-d_{15})	Bioruler	Cat#RH136701
2,3′,4,5′,6-Pentachlorobiphenyl (PCB121)	Cambridge Isotope Laboratories	Cat#PCB-121
2,3-Benzoperylene-d_{14} (perylene-d_{14})	AccuStandard	Cat#B204902
D_4- Bis(2-ethylhexyl) phthalate (DEHP-d_4)	ANPEL Laboratory	Cat#CDAA-320013D4
$^{13}C_4$-perfluorooctane sulfonate (^{13}C-PFOS)	Wellington Laboratories	Cat#MPFCA-MXA
$^{13}C_4$-perfluorooctanoate (^{13}C-PFOA)	Wellington Laboratories	Cat#MPFCA-MXA
Reagents		
Methanol	Thermo Fisher Scientific	Cat#A452-4
Acetonitrile	Thermo Fisher Scientific	Cat#A998-4
Hexane	Adamas	Cat#01226748
Dichloromethane	Adamas	Cat#01226780
Sodium sulfate	Acros	Cat#C19410
Tetra-n-butyl ammonium hydrogen sulfate (TBAS)	Energy Chemical	Cat#A01A0100220250
Sodium carbonate (Na_2CO_3)	Sigma-Aldrich	Cat#V900801

Ammonium acetate	Dima-Tech	Cat#50138
Formic acid	Dikma Technology	Cat#50144
Methyl *tert*-butyl ether	Aladdin Reagent	Cat#B108115
Chloroform	Xilong Scientific	Cat#QC2182
Dimethyl sulfoxide	Aladdin Reagent	Cat#D103273
PBS (pH of 7.4)	Thermo Fisher Scientific	Cat#C10010500BT
O-dianisidine	Sigma-Aldrich	Cat#D3252
Methyl cellulose	Sigma-Aldrich	Cat#M6385
Paraformaldehyde	Sigma-Aldrich	Cat#158127
Ethanol	Aladdin Reagent	Cat#E111962
Phenylhydrazine	Aladdin Reagent	Cat#P108563
Enzyme-linked immunosorbent assay (ELISA) kit for zebrafish		
Zebrafish LPLAT ELISA kit	Meibiao Biotechnology	Cat#MB-21297A
Zebrafish LCLAT ELISA kit	Meibiao Biotechnology	Cat#MB-21311A
Zebrafish PLA_2 ELISA kit	Meibiao Biotechnology	Cat#MB-21294A
Zebrafish CLS ELISA kit	Meibiao Biotechnology	Cat#MB-21278A
Zebrafish XOD ELISA kit	Meibiao Biotechnology	Cat#MB-21290A
Zebrafish TAZ protein ELISA kit	Meibiao Biotechnology	Cat#MB-21296A
Zebrafish ACA-IgA ELISA kit	Meibiao Biotechnology	Cat#MB-21220A
Zebrafish ACA-IgG ELISA kit	Meibiao Biotechnology	Cat#MB-21233A
Zebrafish ACA-IgM ELISA kit	Meibiao Biotechnology	Cat#MB-21228A
Zebrafish PGI_2 ELISA kit	Meibiao Biotechnology	Cat#MB-21260A
Zebrafish TXA_2 ELISA kit	Meibiao Biotechnology	Cat#MB-21262A
Hematoxylin and eosin (H&E) kit	Yihe Biological	Cat#517-28-2; Cat#YH00606
Metabolite standards		
Optimization of screening method, metabolite identification and validation		
16:0 D31-18:1 Phosphatidylcholine (D-PC)	Avanti Polar Lipids	Cat#860399
14:1-14:1 Phosphatidylcholine (PC)	Avanti Polar Lipids	Cat#330708
16:0 D31-18:1 Phosphatidylethanolamine (D-PE)	Avanti Polar Lipids	Cat#860374
14:1-14:1 Phosphatidylethanolamine (PE)	Avanti Polar Lipids	Cat#330708
16:0 D31-18:1 Phosphatidylserine (D-PS)	Avanti Polar Lipids	Cat#860403
14:1-14:1 Phosphatidylserine (PS)	Avanti Polar Lipids	Cat#330708
16:0 D31-18:1 Phosphatidylinositol (D-PI)	Avanti Polar Lipids	Cat#860042
14:1-14:1 Phosphatidylinositol (PI)	Avanti Polar Lipids	Cat#330708
16:0 D31-18:1 Phosphatidylglycerol (D-PG)	Avanti Polar Lipids	Cat#860384

14:1-14:1 Phosphatidylglycerol (PG)	Avanti Polar Lipids	Cat#330708
18:1 Lysophosphatidylcholine (LPC)	Avanti Polar Lipids	Cat#845875
14:1 Diacylglycerol (DG)	Avanti Polar Lipids	Cat#330708
D-erythro-sphingosine-d7 (D-Sph)	Avanti Polar Lipids	Cat#860657
D-erythro-Sphingosine (Sph)	Avanti Polar Lipids	Cat#860490
16:0-D31 Ceramide (D-Cer)	Avanti Polar Lipids	Cat#868516
18:1-18:1 Ceramide (Cer)	Avanti Polar Lipids	Cat#860519
18:1-18:1 Sphingomyelin (SM)	Avanti Polar Lipids	Cat#860587
16:0-D31 Sphingomyelin (D-SM)	Avanti Polar Lipids	Cat#868584
18:1-17:0 Glucosylceramide (GlcCer)	Avanti Polar Lipids	Cat#860569
18:1-18:1 Lactosylceramide (LacCer)	Avanti Polar Lipids	Cat#860596
18:1-12:0 Sulfatide (Sul)	Avanti Polar Lipids	Cat#860573
Ganglioside GM3 (d40:1)	Avanti Polar Lipids	Cat#860058
Ganglioside GM3 (d38:1)	Avanti Polar Lipids	Cat#860058
Ganglioside GM3 (d39:1)	Avanti Polar Lipids	Cat#860058
Ganglioside GM3 (d41:1)	Avanti Polar Lipids	Cat#860058
Ganglioside GM3 (d42:1)	Avanti Polar Lipids	Cat#860058
Ganglioside GM1 (d36:1)	Qilu Pharmaceutical	AN#H20046213
Ganglioside GM1 (d38:1)	Qilu Pharmaceutical	AN#H20046213
Ganglioside GD3 (d34:1)	Avanti Polar Lipids	Cat#860060
Metabolite identification and validation		
Cardiolipin (CL, 18:1)	Avanti Polar Lipids	Cat#710335P
Cardiolipin (CL, 14:0)	Avanti Polar Lipids	Cat#750332P
Cardiolipin (CL, 16:0)	Avanti Polar Lipids	Cat#710333P
Sepiapterin (Sep)	Toronto Research Chemicals	Cat#S258913
Isoxanthopterin (ISO)	Cayman Chemical	Cat#17564
Neopterin (Neo)	Cayman Chemical	Cat#12057
Folate (VB_9)	Sigma-Aldrich	Cat#47866
Pyridoxine (VB_6)	Sigma-Aldrich	Cat#P5669
Nicotinic acid (VB_3)	Sigma-Aldrich	Cat#47864
Guanine	Sigma-Aldrich	Cat#PHR1243
Mesaconic acid (Mesaconate)	Sigma-Aldrich	Cat#131040
2-Amino-Succinic acid 4-Ethyl Ester	Sigma-Aldrich	Cat#S334383
L-(-)-Malic acid (Malate)	Sigma-Aldrich	Cat#09172
L-Threonate	Toronto Research Chemicals	Cat#T404990
L-Aspartate	Sigma-Aldrich	Cat#51572
UDP-α-D-Glucose	Biosynth	Cat#15602
Nicotinamide Adenine Dinucleotide (NAD^+)	Cayman Chemical	Cat#16077

UDP-N-acetyl-D-Glucosamine (UDP-GlcNAc)	Cayman Chemical	Cat#20353
Cholate (BAs)	ANPEL Laboratory	Cat#CDAA263004
L-Cystathionine	Cayman Chemical	Cat#16061
Betaine	Toronto Research Chemicals	Cat#B325005
Stearidonoyl glycine	Cayman Chemical	Cat#9000327
L-Pyroglutamic acid (5-Oxoproline)	Sigma-Aldrich	Cat#83160
DL-β-Leucine (β-Leucine)	Sigma-Aldrich	Cat#L8000
L-Glutamate	Dr. Ehrenstorfer GmbH	Cat#C14034400
L-Tyrosine	Sigma-Aldrich	Cat#91515
Phenylpyruvic acid (Phenyl-pyruvate)	Sigma-Aldrich	Cat#74346
L-Phenylalanine (Phenylalanine)	Sigma-Aldrich	Cat#P2126
L-Glutathione Oxidized (GSSG)	Sigma-Aldrich	Cat#V900363
L-Histidine	Sigma-Aldrich	Cat#73767
L-Tryptophan	Sigma-Aldrich	Cat#T0254
2-Aminobenzimidazole (BAMs)	Sigma-Aldrich	Cat#31189
1-(2-Pyrimidyl) piperazine (BAMs)	Sigma-Aldrich	Cat#421235
2,4-Dimethylbenzaldehyde	Sigma-Aldrich	Cat#8.21461.0010
β-Carotene	Sigma-Aldrich	Cat#PHR1239
Adenosine 5'-Monophosphate (AMP)	Toronto Research Chemicals	Cat#A281780
Inosine-5'-Monophosphate (IMP)	Toronto Research Chemicals	Cat#I665005
Adenosine 5'-Diphosphate (ADP)	Cayman Chemical	Cat#16778
Adenosine 5'-Triphosphate (ATP)	Sigma-Aldrich	Cat#A1852
18:1 Lysophosphatidylinositol (LPI)	Avanti Polar Lipids	Cat#850100P
Octadecyl Amine	Sigma-Aldrich	Cat#74750
Nonanoic acid	Larodan	Cat#10-0900-9
Homogamma-Linolenic acid (Diho-γ-Lin)	Larodan	Cat#10-2013-7
Gamma-Linolenic acid (γ-Lin)	Larodan	Cat#10-1830-9
Linoleate (Lin)	Larodan	Cat#10-1802-13
α-linoleate (α-Lin)	Yuanye Bio-Technology	Cat#B21967
Eicosapentaenoic acid (EPA)	Larodan	Cat#10-2005-7
Arachidonate (Ara)	Larodan	Cat#10-2004-7
Rescue experiments		
Linoleate (Lin)	Larodan	Cat#10-1802-13
Arachidonate (Ara)	Larodan	Cat#10-2004-7
α-linoleate (α-Lin)	Yuanye Bio-Technology	Cat#B21967
Isoxanthopterin (ISO)	Cayman Chemical	Cat#17564

Isotope tracing		
Linoleate (Lin)	Larodan	Cat#10-1802-13
^{13}C-labeled linoleate (^{13}C-Lin)	Toronto Research Chemicals	Cat#L467500
Software		
Progenesis QI 2.3	Waters	http://www.nonlinear.com/progenesis/qi/
Compound Discoverer 2.1	Thermo Fisher	https://planetorbitrap.com/compound-discoverer
Gephi 0.9.2	Gephi	https://gephi.org/
NIS-Elements D3.10	Nikon	https://www.nikon.com/products/microscope-solutions/lineup/img_soft/nis-elements/
SPSS	IBM	https://www.ibm.com/analytics/spss-statistics-software

Table S2. The major affected metabolic processes, including major metabolites with statistically different levels compared with those of the control group and the corresponding exposure chemicals. All listed endogenous metabolites were identified and validated with referenced standards.

Region	Metabolic process	Affected metabolites	Effective chemicals	Effects
I	Cardiolipin biosythesis	Cardiolipin	p,p'-DDE, TPHP, PFOS, TCS	Increase
	Lysophospholipid metabolism	LPC, LPE	p,p'-DDE, TPHP, PFOS, TCS	Decrease
	Metabolism of cofactors and vitamins	Isoxanthopterin; Vitamin B_6 analogue, Vitamin B_3 analogue	TCS	Decrease
	Glycerophospholipid metabolism	PE, PS	p,p'-DDE, TPHP, PFOS, TCS	Decrease
		PC, PE, PS, PI	p,p'-DDE, TPHP, PCB153, TPT	Increase
	Bile acid biosynthesis	5β-Cyprinosulfate, 5β-Cyprinosulfate-OH, Cholestane-pentol	p,p'-DDE, TPHP, PCB153, TPT, BPA, 6OHBDE47, TCS, PFOS, PFOA	Decrease
	Fatty acid biosynthesis	Linoleate, γ-Linoleate, Dihomo-γ-Linoleate, Arachidonate, Adrenic acid, Eicosanoic acid, 11,12-EET, α-Linoleate, EPA, DPA, α-Eleostearic acid, Hexadecenoic acid	p,p'-DDE, TPHP, PFOS, TCS, BPA, PCB153, TPT	Decrease
II	Amino acids metabolism	L-Cystathione, Betaine, N-Methylglycine, Stearidonoyl glycine, Phenyl-alanine, Phenyl-pyruvate, 5-Oxoproline, GSSG, L-Glutamine, L-Histidine	p,p'-DDE, TPHP, POFS, 6OHBDE47, PCB153, TPT	Decrease
	Nucleotide metabolism	Hypoxanthine, Guanine, Purines	p,p'-DDE, TPHP, PFOS, 6OHBDE47, PCB153, TPT	Decrease
		Pyrimidines	TCS, DEHP PFOS, p,p'-DDE, TPHP	Decrease Increase
	Acylamide biosynthesis	Peptides	p,p'-DDE, TPHP	Increase
	Secondary metabolites biosynthesis	O-Heterocyclic compounds, N-Heterocyclic compounds	p,p'-DDE, PFOS, PFOA, TCS, BPA, B(a)P, DEHP	Increase

Table S3. Optimized instrumental and MRM conditions of the target chemicals.

Analyte	MRM transition	Cone voltage (kV)	Collision energy (eV)
BPA	227.10 > 211.95	38.0	18.0
	227.10 > 132.90	38.0	28.0
6OHBDE47	500.63 > 78.46	16.0	14.0
	500.63 > 81.32	16.0	22.0
TCS	286.85 > 34.99	18.0	4.0
	286.85 > 141.95	18.0	28.0
	288.85 > 34.99	18.0	4.0
^{13}C-BPA	229.13 > 212.92	38.0	18.0
	229.13 > 134.96	38.0	28.0
PFOS	498.83 > 98.74	5.0	44.0
	498.83 > 129.76	5.0	44.0
	498.83 > 79.82	5.0	56.0
^{13}C-PFOS	502.94 > 98.96	5.0	44.0
	502.94 > 79.82	5.0	56.0
PFOA	412.88 > 368.79	4.0	10.0
	412.88 > 218.80	4.0	16.0
	412.88 > 168.82	4.0	18.0
^{13}C-PFOA	416.90 > 221.99	4.0	16.0
	416.90 > 168.95	4.0	18.0
DEHP	391.06 > 70.98	18.0	8.0
	391.06 > 166.87	18.0	12.0
DEHP-d_4	395.23 > 171.04	12.0	12.0
	395.23 > 152.97	12.0	36.0
TPHP	326.97 > 214.92	42.0	24.0
	326.97 > 76.90	42.0	46.0
	326.97 > 151.87	42.0	46.0
TPT	428.86 > 350.85	40.0	18.0
	350.90 > 196.79	72.0	24.0
	350.90 > 119.75	72.0	28.0
TPHP-d_{15}	342.04 > 81.98	18.0	42.0

Table S4. List of materials and calibration standards in the kits.

Reagents	Amount needed for 96 samples
Standards (for Different Indicators)	0.3 mL x 6 tubes
Sample Diluent	6.0 mL
HRP-Conjugate Reagent	10.0 mL
20X Wash Solution	25.0 mL
Chromogen Solution A	6.0 mL
Chromogen Solution B	6.0 mL
Stop Solution	6.0 mL
ELISA Kit for Zebrafish	Standard concentration (from S_0 to S_5)
LPLAT	0, 50, 100, 200, 400, 800 U/L
LCLAT	0, 30, 60, 120, 240, 480 U/L
PLA_2	0, 3, 6, 12, 24, 48 U/L
CLS	0, 25, 50, 100, 200, 400 U/L
XOD	0, 0.25, 0.5, 1, 2, 4 U/L
TAZ	0, 2.5, 5, 10, 20, 40 ng/mL
ACA-IgA	0, 3, 6, 12, 24, 48 APL U/mL
ACA-IgG	0, 3, 6, 12, 24, 48 GPL U/mL
ACA-IgM	0, 3, 6, 12, 24, 48 MPL U/mL
PGI_2	0, 10, 20, 40, 80, 160 pg/mL
TXA_2	0, 15, 30, 60, 120, 240 pg/mL

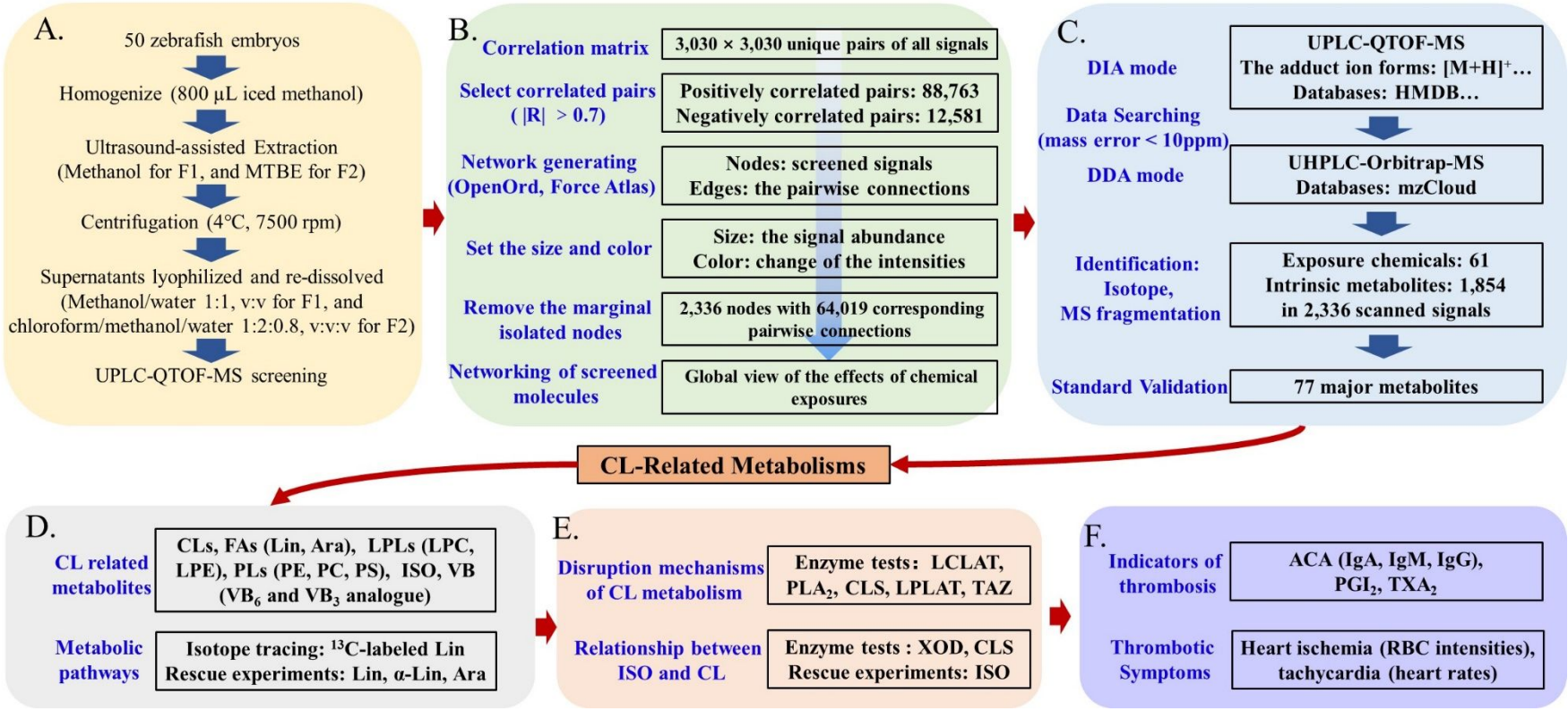

Figure S1. A workflow diagram of this study.

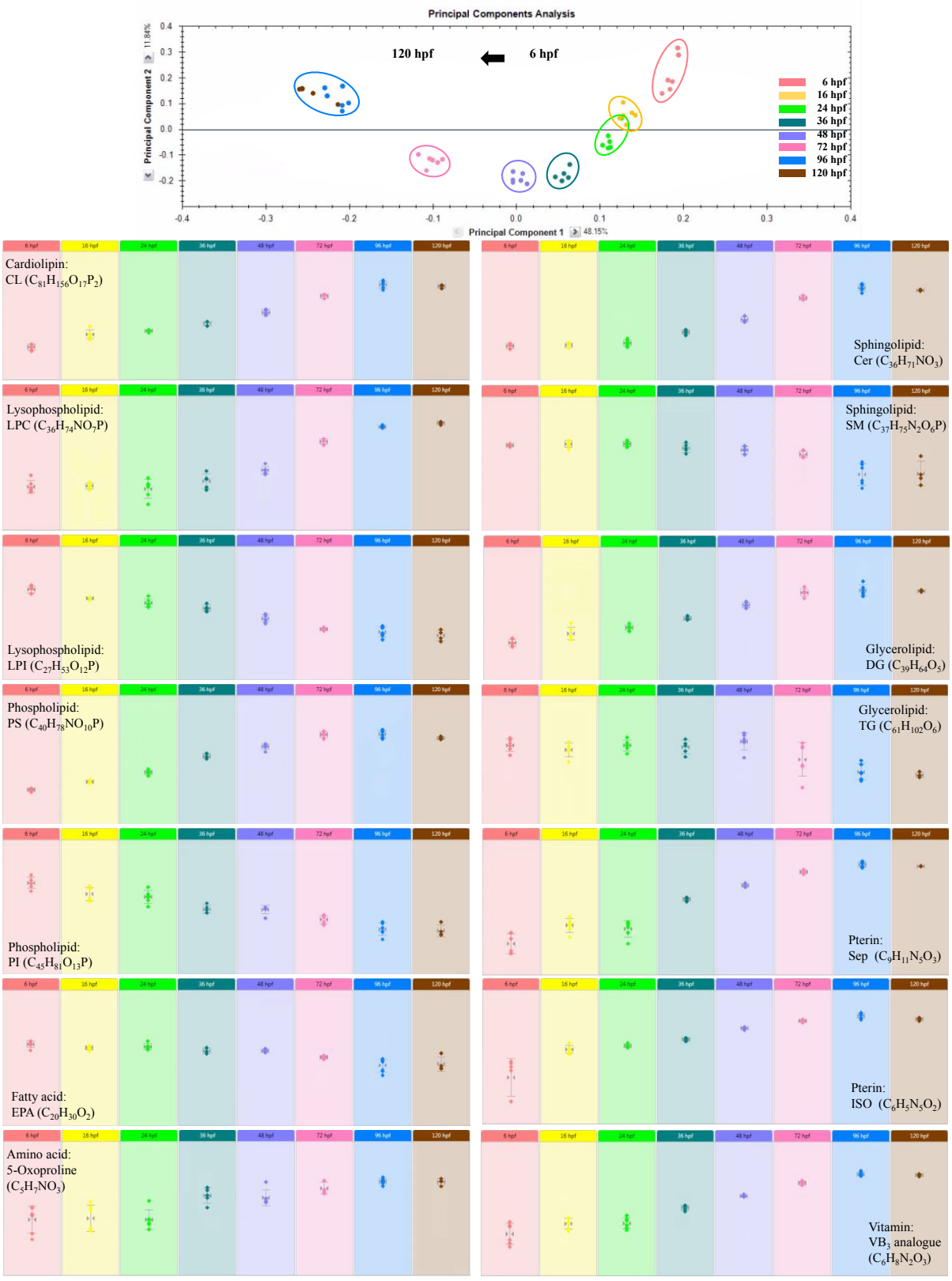

Figure S2. PCA analysis of screened metabolites during the developing stages of zebrafish embryos (6 to 120 h post fertilization), and concentration changes of representative molecules of the screened metabolites.

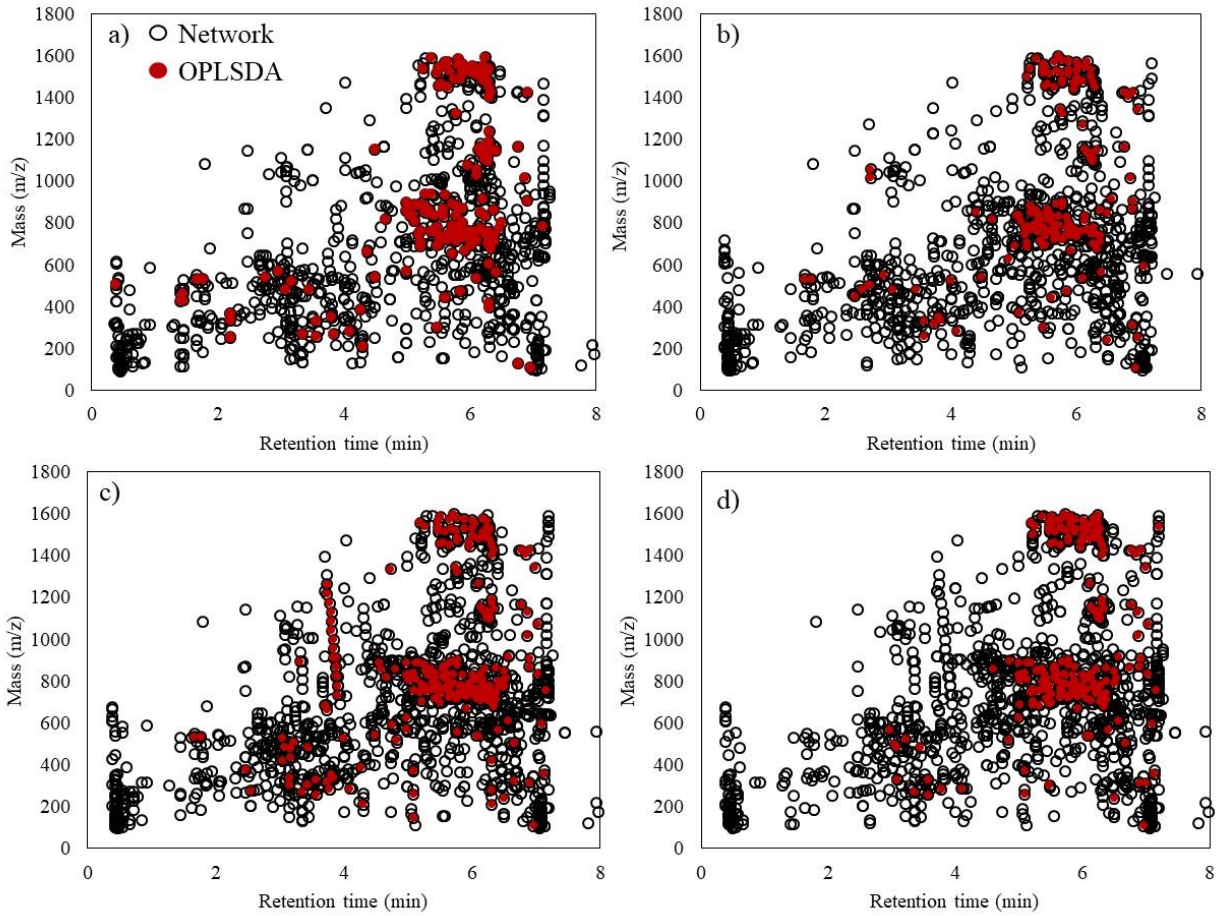

Figure S3. Selected molecules obtained by network analysis and OPLSDA exemplified by zebrafish embryos exposed to TCS (a), PFOS (b), pp´-DDE (c), and TPHP (d).

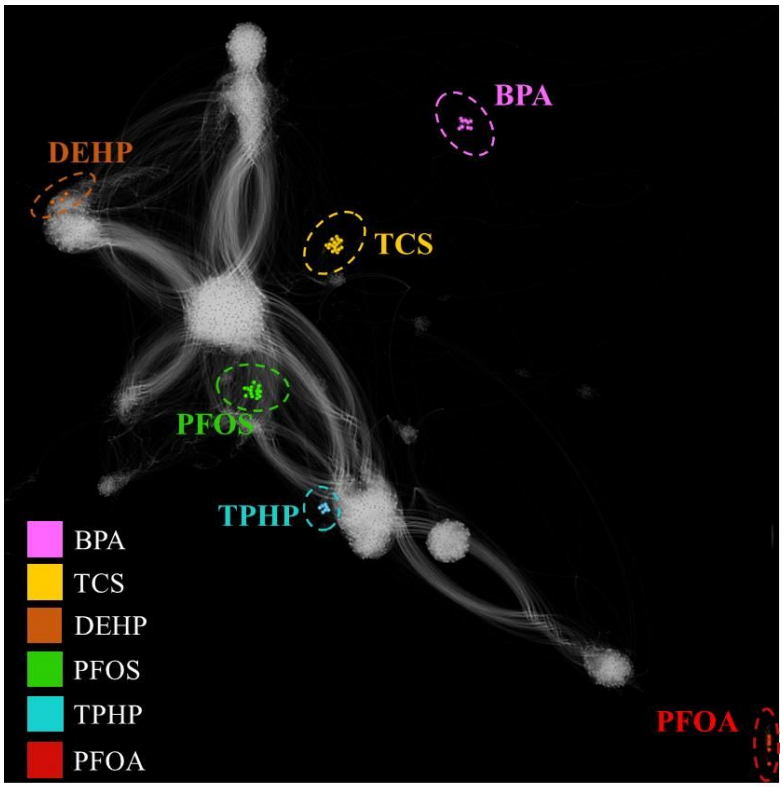

Figure S4. Distributions of exposure chemicals and their metabolites detected in the auto-generated network.

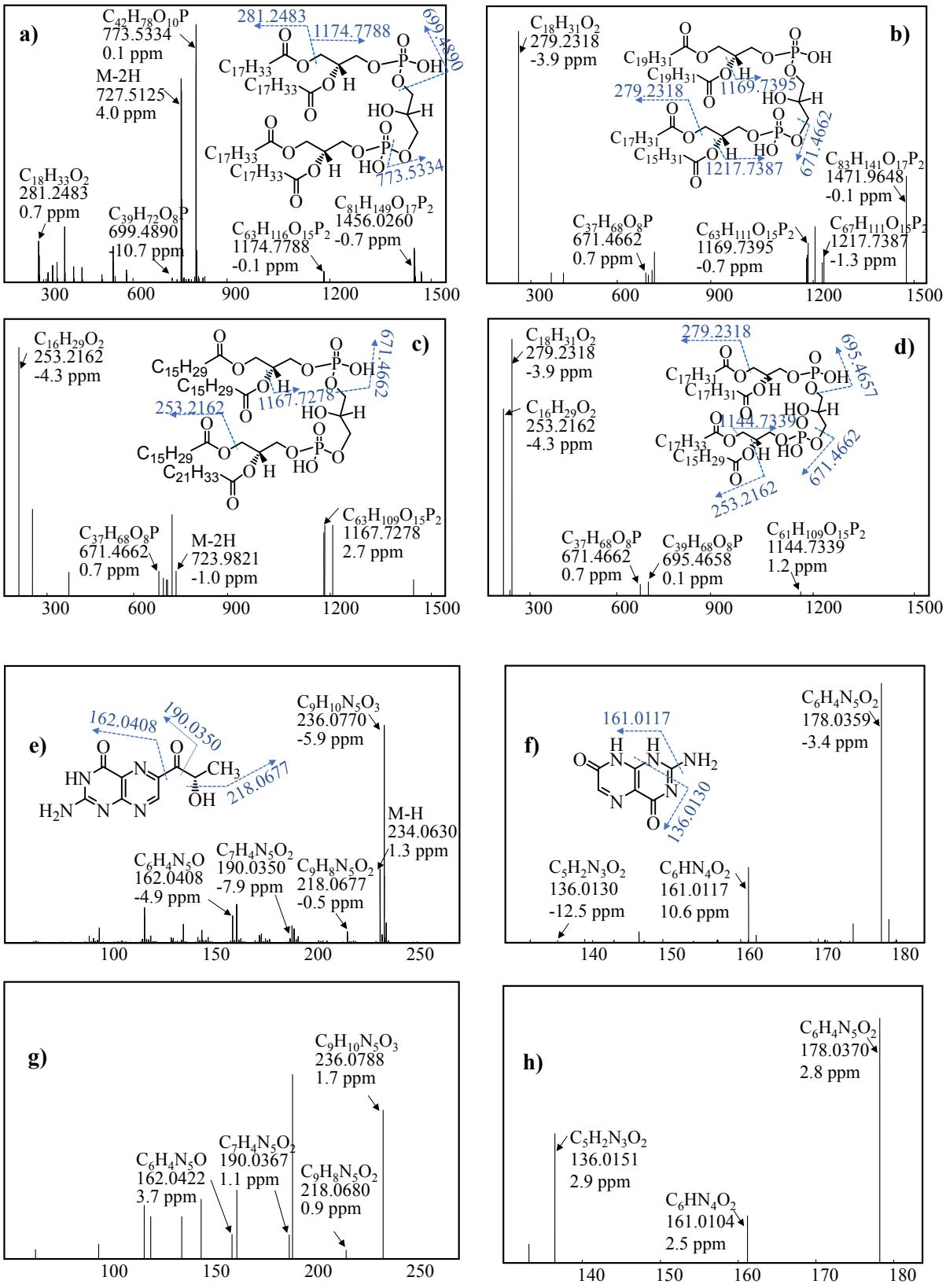

Figure S5. Mass spectra of standards of CL (a: $C_{81}H_{149}O_{17}P_2$), Sep (e), and ISO (f). Mass spectra of CLs (b: $C_{83}H_{142}O_{17}P_2$, c: $C_{79}H_{138}O_{17}P_2$, d: $C_{79}H_{142}O_{17}P_2$), Sep (g), and ISO (h) detected in zebrafish embryo.

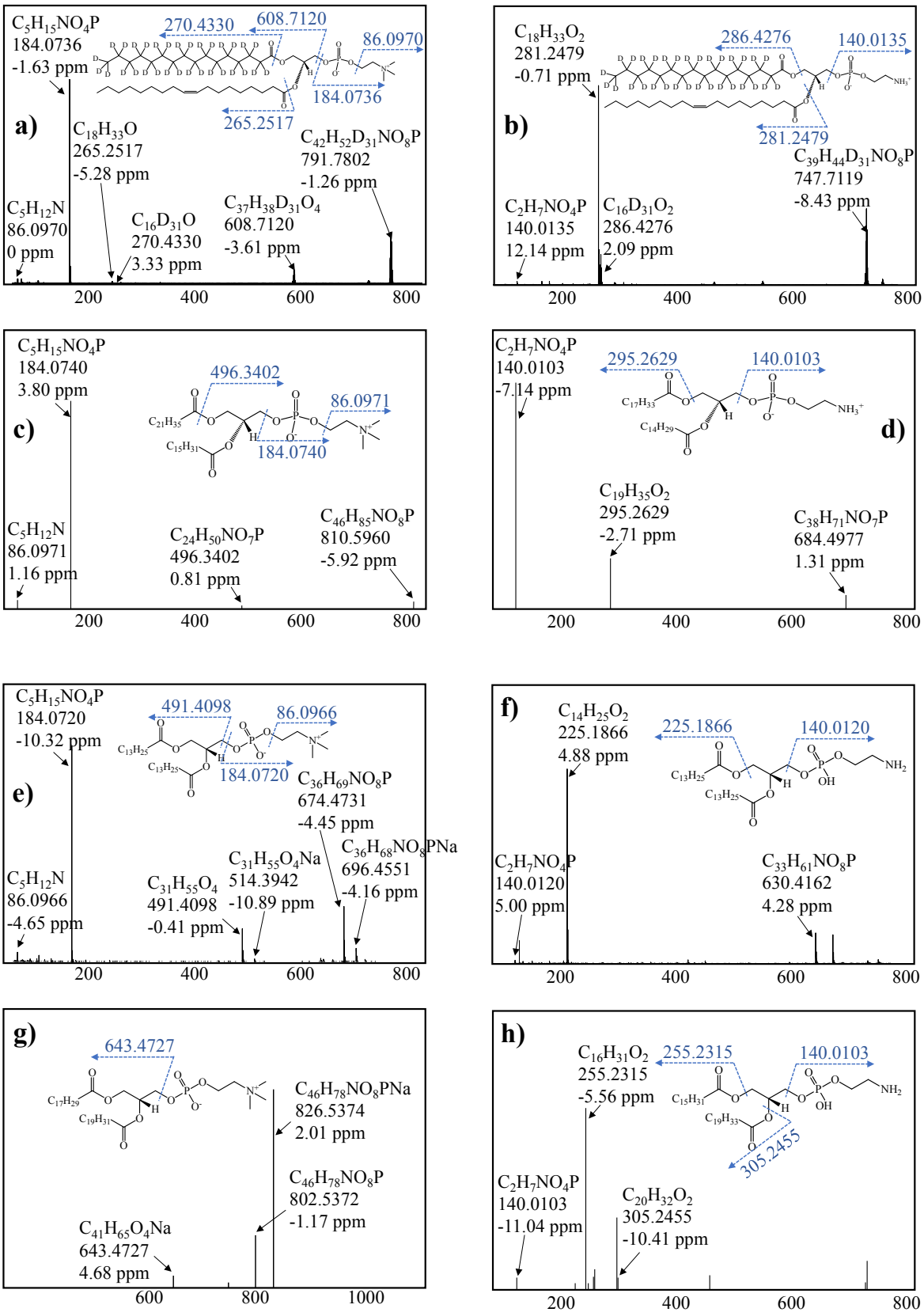

Figure S6. Mass spectra of standards of D-PC (a), D-PE (b), PC (e), and PE (f). Mass spectra of PC (c: $C_{46}H_{84}NO_8P$, g: $C_{46}H_{78}NO_8P$) and PE (d: $C_{38}H_{74}NO_8P$, h: $C_{41}H_{76}NO_8P$) detected in zebrafish embryo.

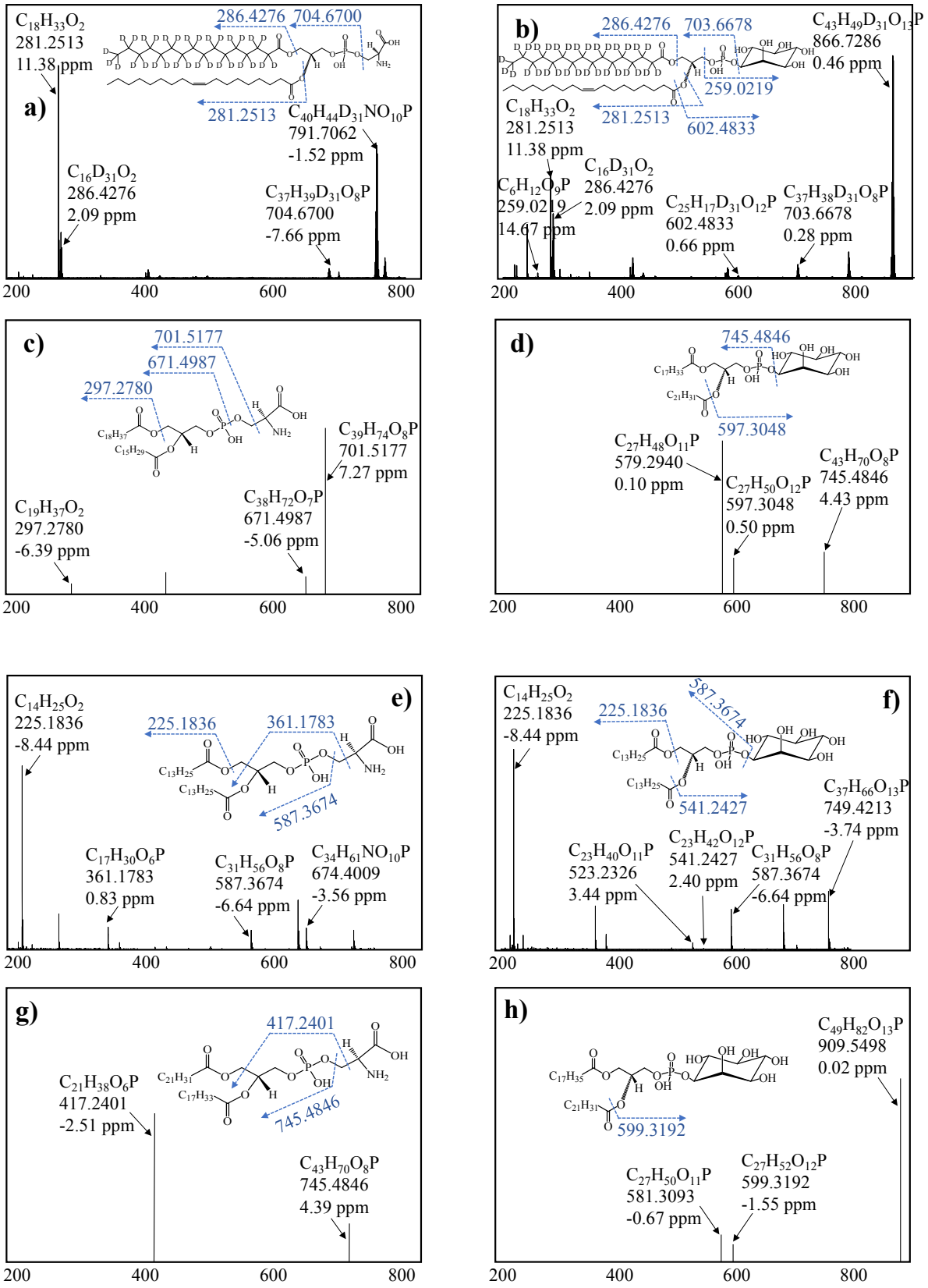

Figure S7. Mass spectra of standards of D-PS (a), D-PI (b), PS (e), and PI (f). Mass spectra of PS (c: $C_{41}H_{78}NO_{10}P$, g: $C_{46}H_{76}NO_{10}P$) and PI (d: $C_{49}H_{81}O_{13}P$, h: $C_{49}H_{83}O_{13}P$) detected in zebrafish embryo.

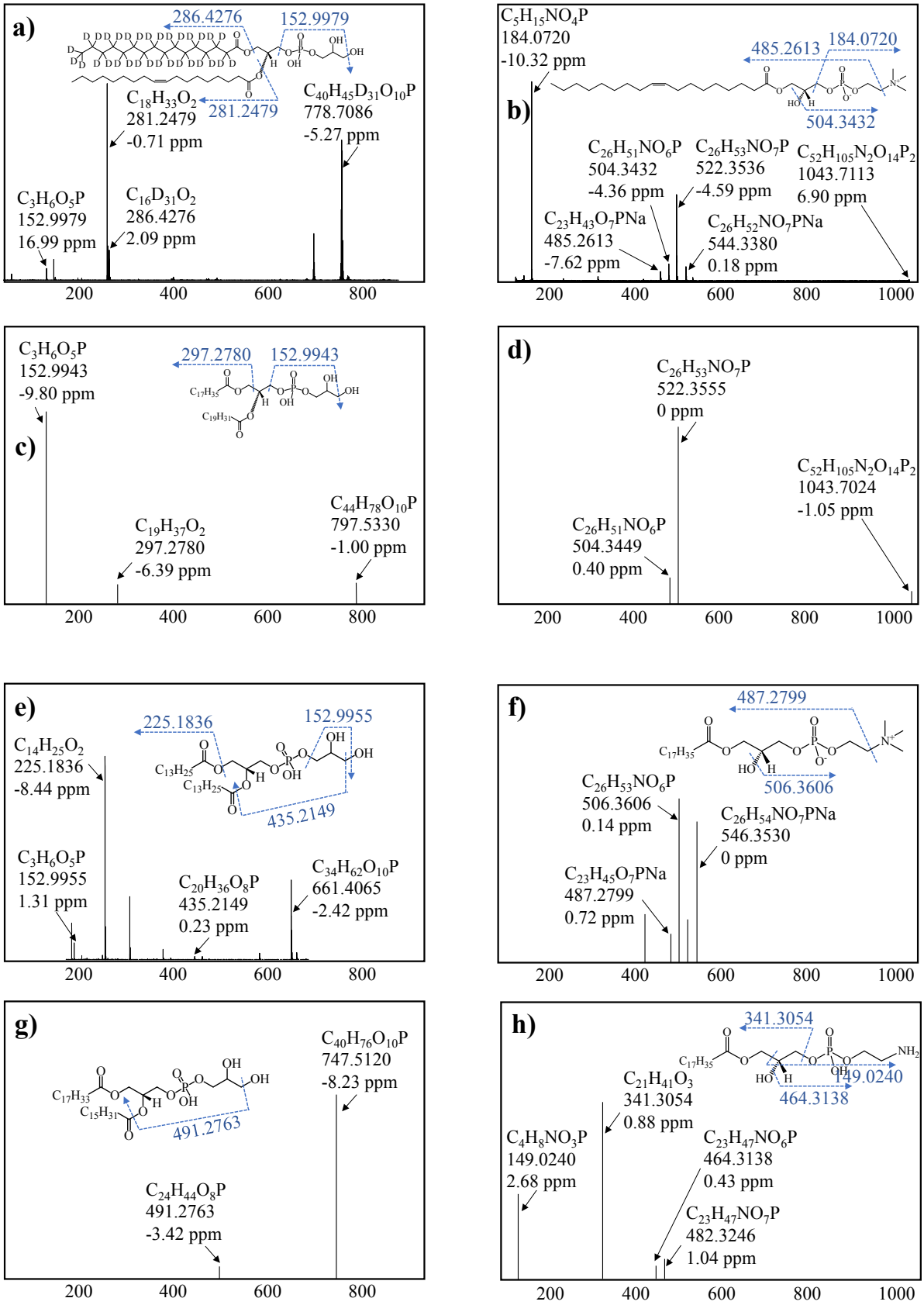

Figure S8. Mass spectra of standards of D-PG (a), LPC (b), and PG (e). Mass spectra of PG (c: $C_{44}H_{79}O_{10}P$, g: $C_{40}H_{77}O_{10}P$), LPC (d: $C_{26}H_{52}NO_7P$, f: $C_{26}H_{54}NO_7P$) and LPE (h: $C_{23}H_{48}NO_7P$) detected in zebrafish embryo.

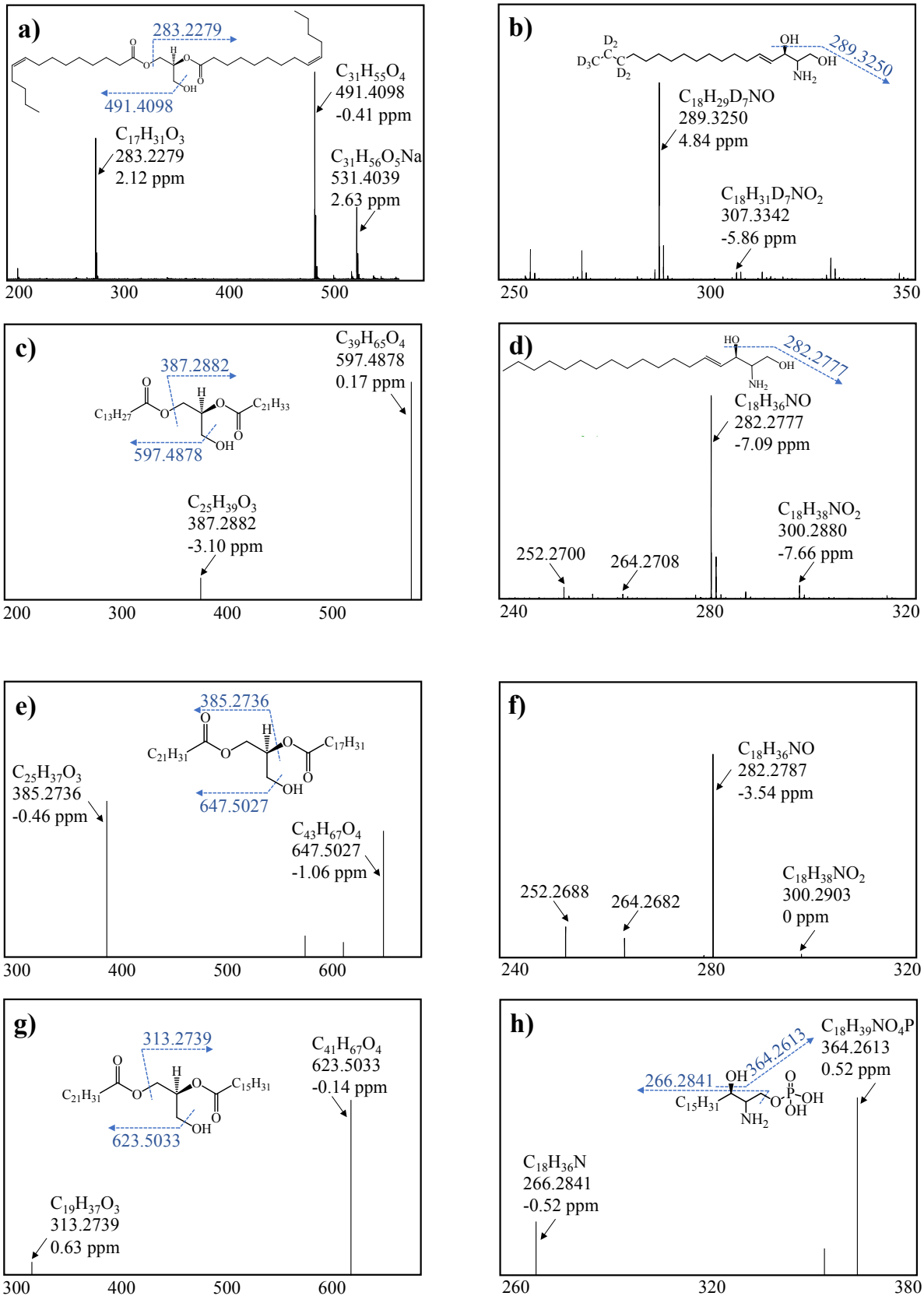

Figure S9. Mass spectra of standards of DG (a), D-Sph (b), and Sph (d). Mass spectra of DG (c: $C_{39}H_{66}O_5$, e: $C_{43}H_{68}O_5$, g: $C_{41}H_{68}O_5$), Sph (f: $C_{18}H_{37}NO_2$) and dhS-1-P (h: $C_{18}H_{40}NO_5P$) detected in zebrafish embryo.

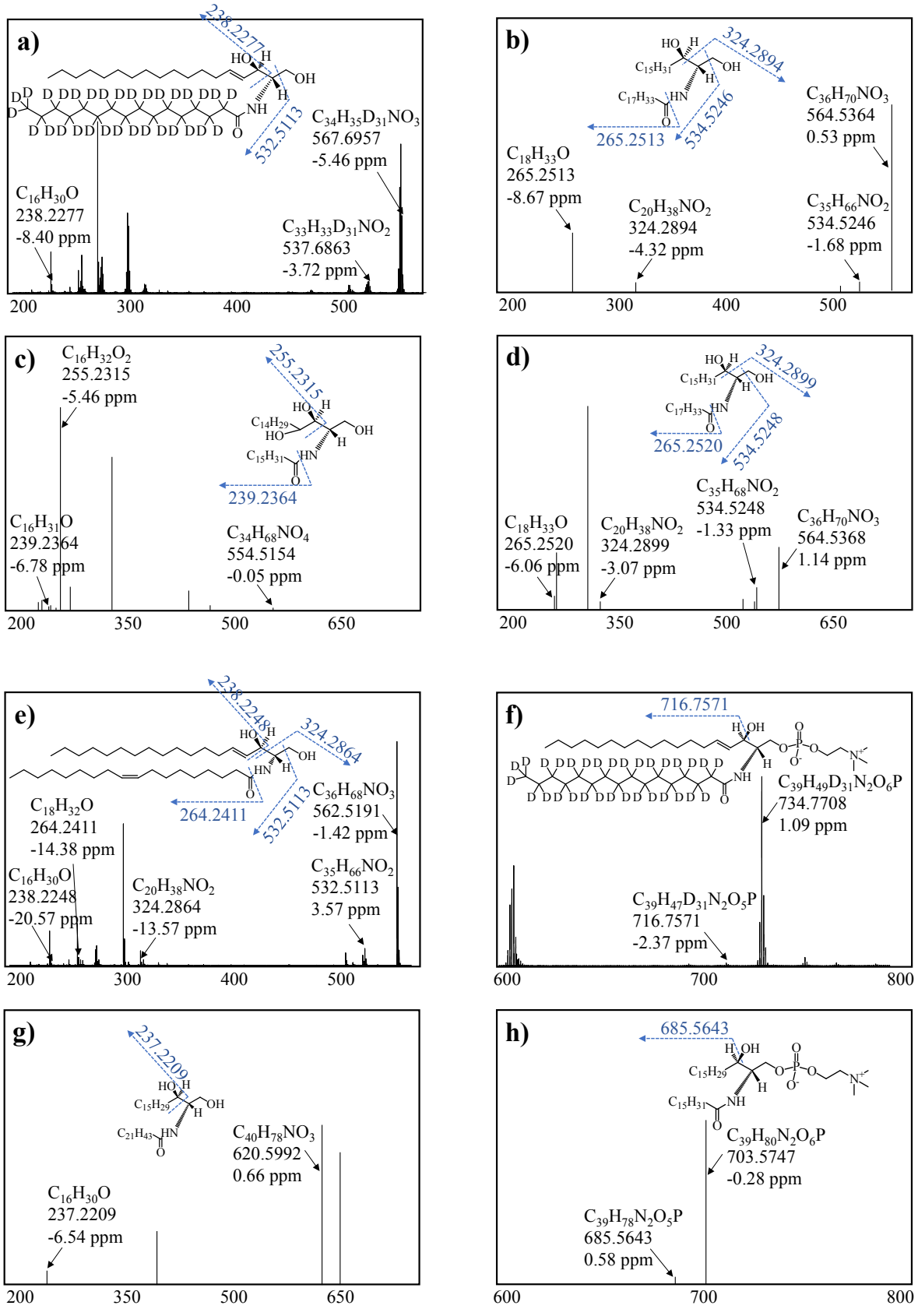

Figure S10. Mass spectra of standards of D-Cer (a), Cer (e), and D-SM (f). Mass spectra of dhCer (b: $C_{36}H_{71}NO_3$, d: $C_{36}H_{71}NO_3$), OH-Cer (c: $C_{34}H_{69}NO_4$), Cer (g: $C_{40}H_{79}NO_3$) and SM (h: $C_{39}H_{79}N_2O_6P$) detected in zebrafish embryo.

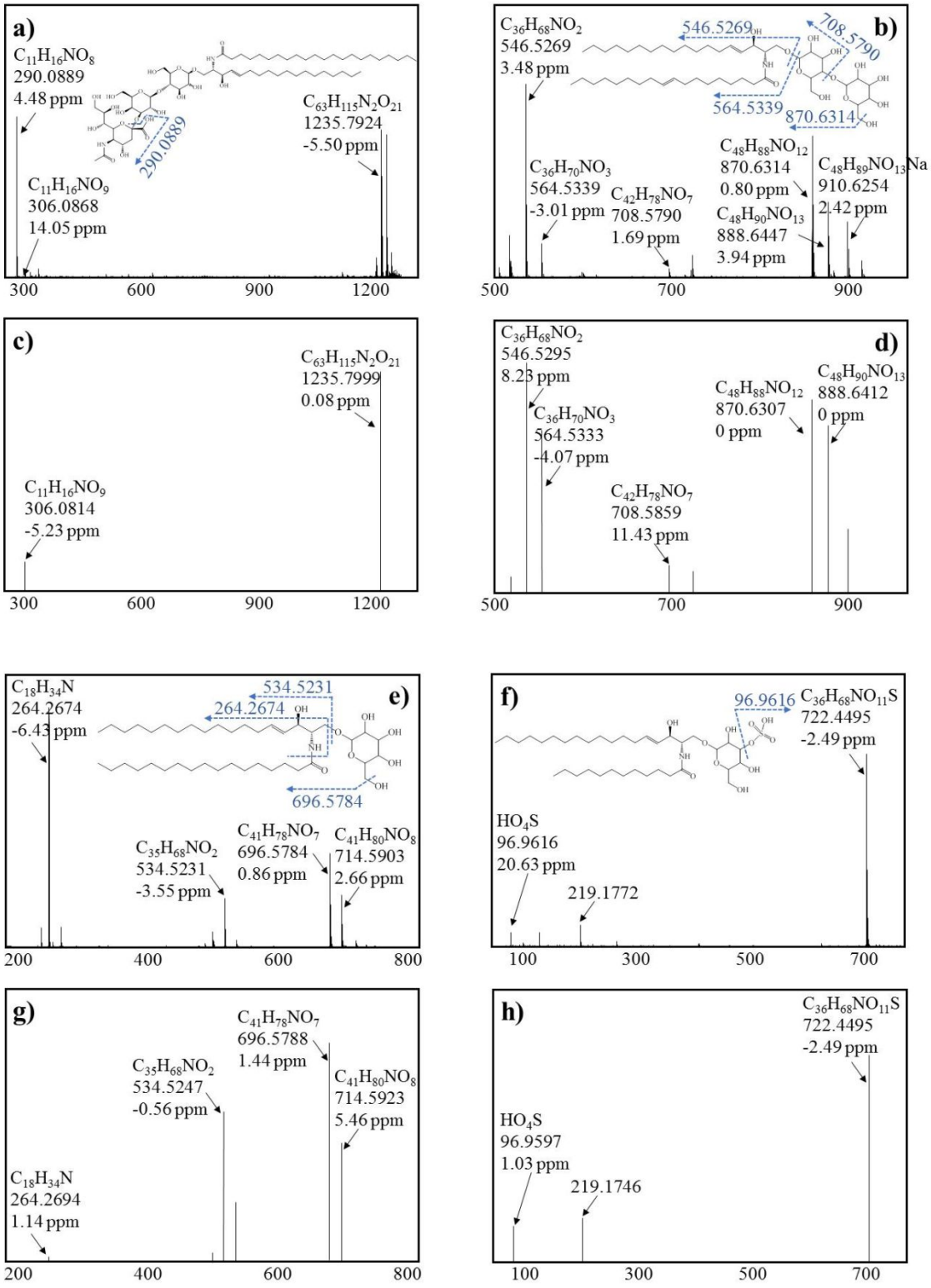

Figure S11. Mass spectra of standards of GM_3 (d40:1) (a), LacCer (b), GlcCer (e) and Sul (f). Mass spectra of GM_3 (c: $C_{63}H_{116}N_2O_{21}$), LacCer (d: $C_{48}H_{89}NO_{13}$), GlcCer (g: $C_{41}H_{79}NO_8$) and Sul (h) detected in zebrafish embryo.

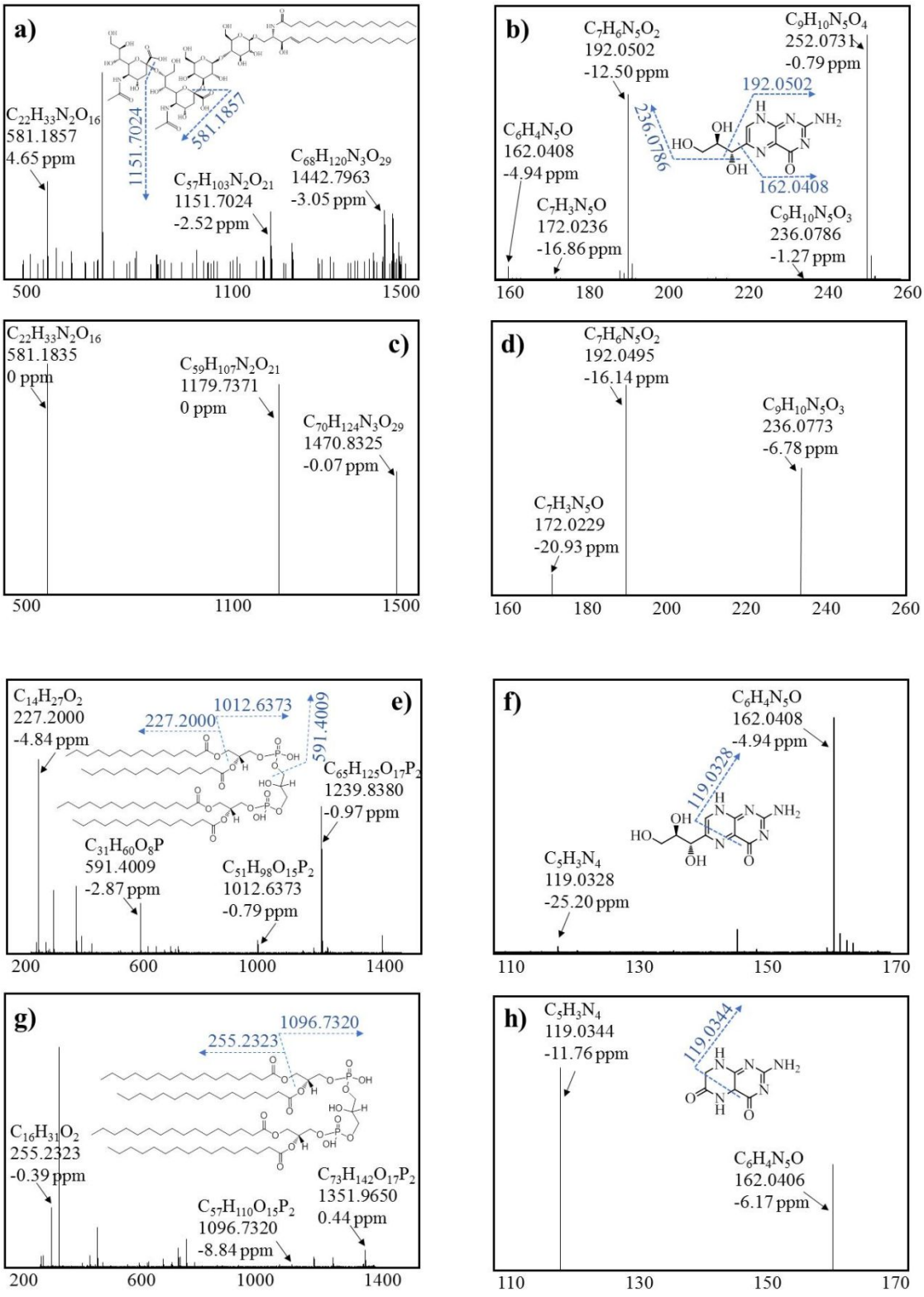

Figure S12. Mass spectra of standards of GD_3 (d34:1) (a), Neo (b, m/z 160-260; f: m/z 110-170), CL (14:0) (e) and CL (16:0) (g). Mass spectra of GD_3 (c: $C_{63}H_{116}N_2O_{21}$), Neo (d), and 7,8-Dihydroxanthopterin (7,8-Dixa) (h) detected in zebrafish embryo. Mass spectra of CLs detected in embryo were shown in Figure 3.

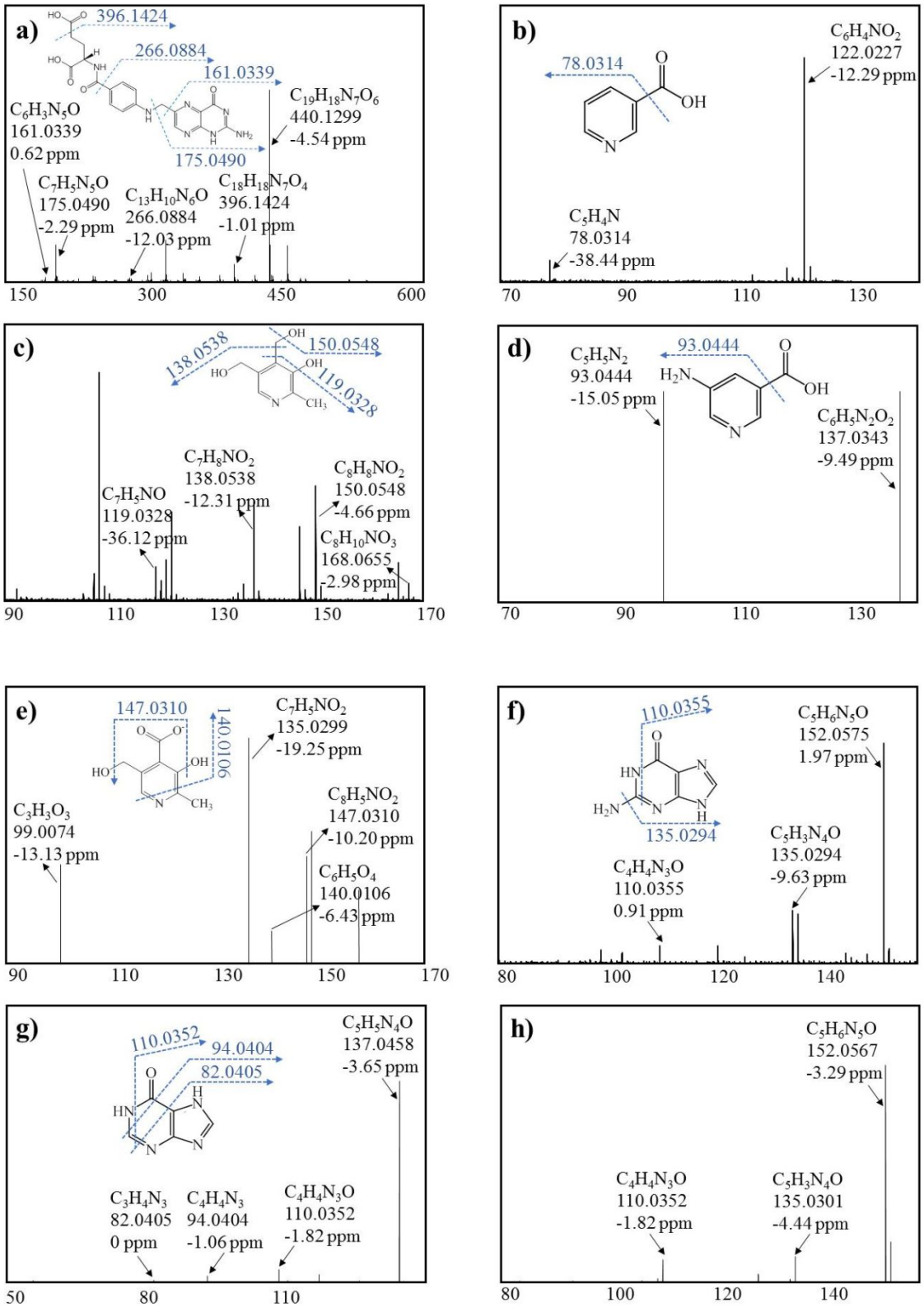

Figure S13. Mass spectra of standards of VB_9 (a), VB_3 (b), VB_6 (c), and Guanine (f). Mass spectra of VB_3 analogue (d), VB_6 analogue (e), Hypoxanthine (g), and Guanine (h) detected in zebrafish embryo.

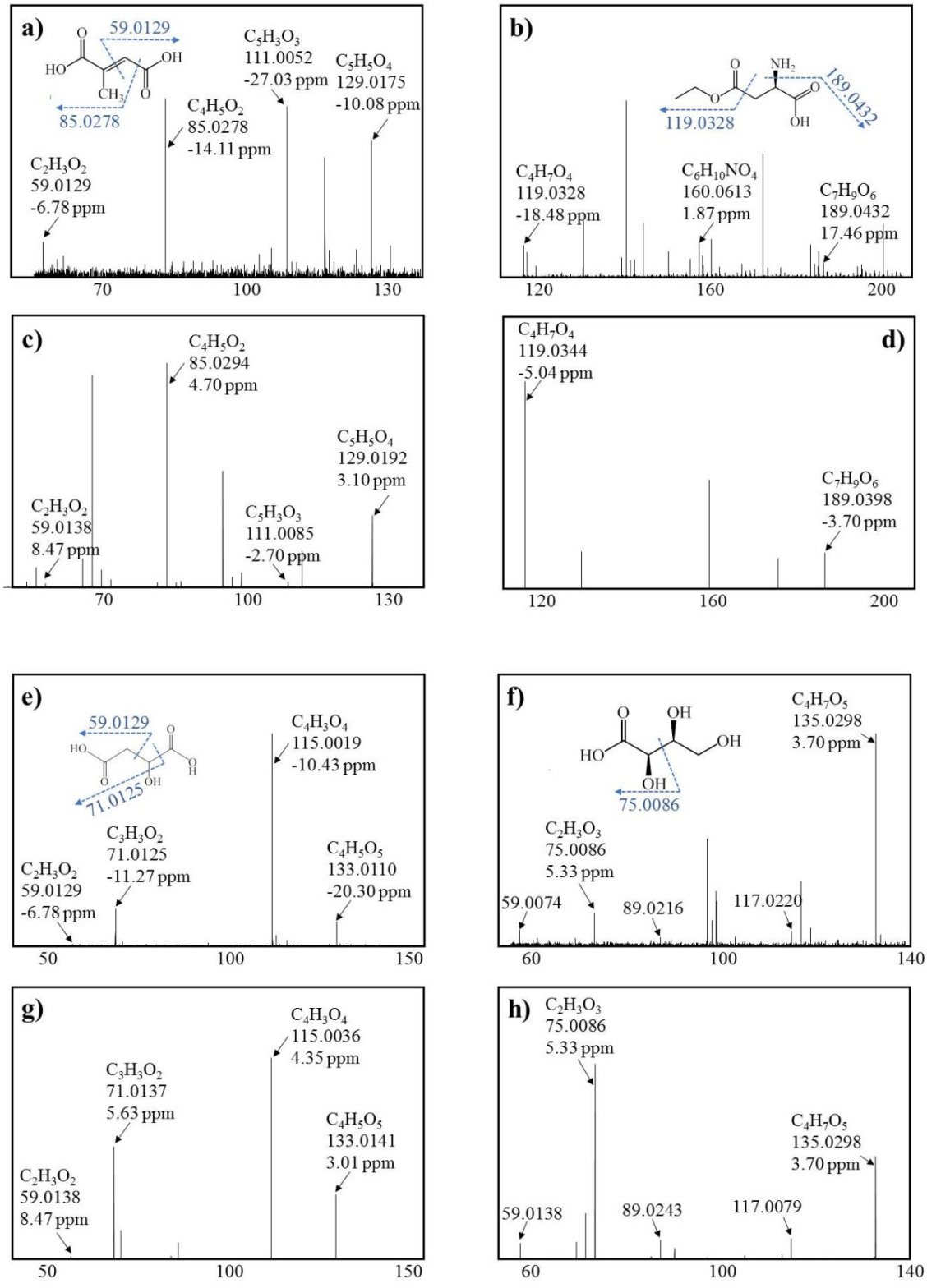

Figure S14. Mass spectra of standards of Mesaconate (a), 2-Amino-Succinic acid-4-Ethyl ester (b), Malate (e), and L-Threonate (f). Mass spectra of Mesaconate (c), 2-Amino-Succinic acid-4-Ethyl ester (d), Malate (g), and L-Threonate (h) detected in zebrafish embryo.

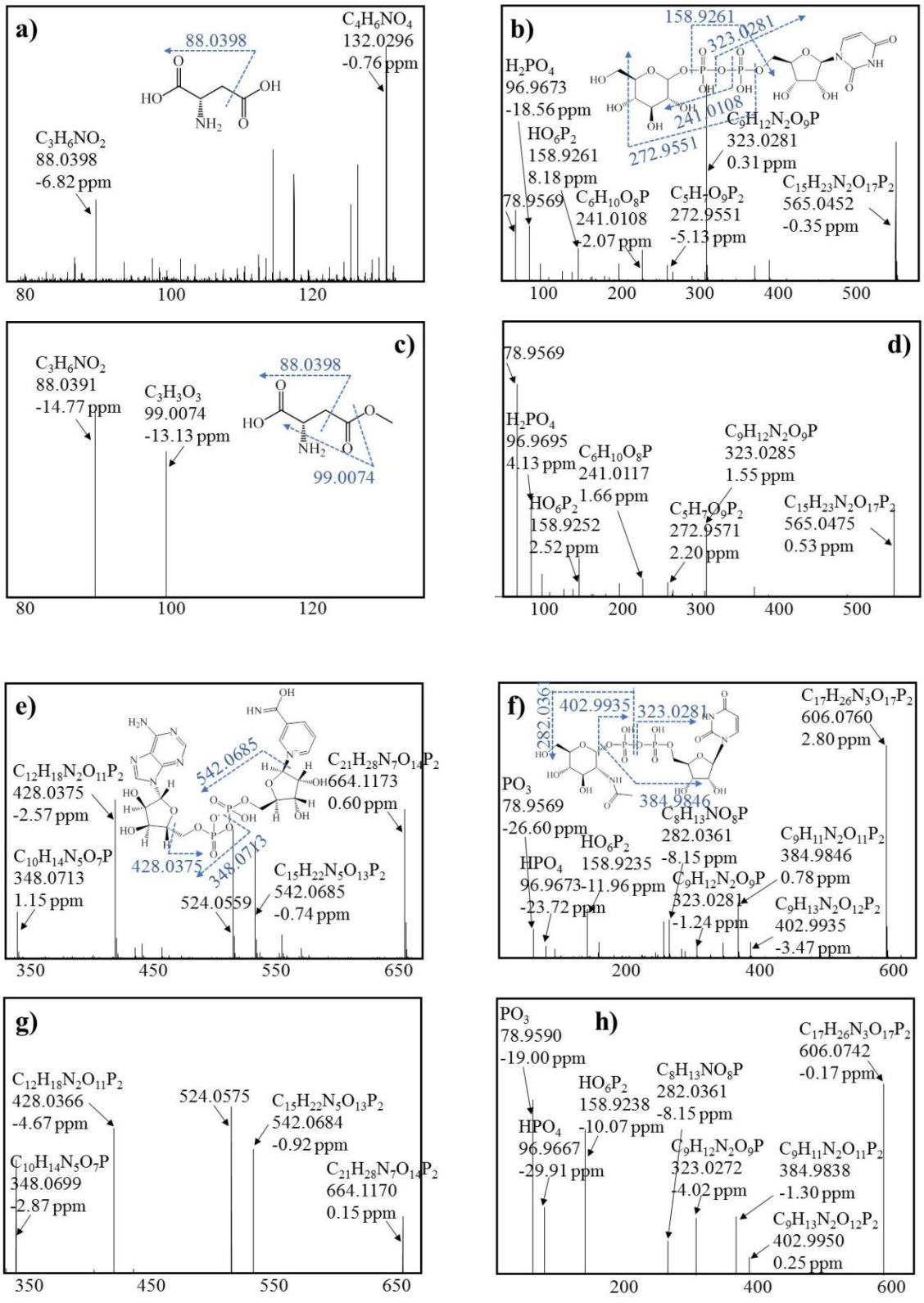

Figure S15. Mass spectra of standards of L-Aspartate (a), UDP-α-D-Glucose (b), NAD^+ (e), and UDP-GlcNAc (f). Mass spectra of H-Asp(OMe)-OH (c), UDP-α-D-Glucose (d), NAD^+ (g), and UDP-GlcNAc (h) detected in zebrafish embryo.

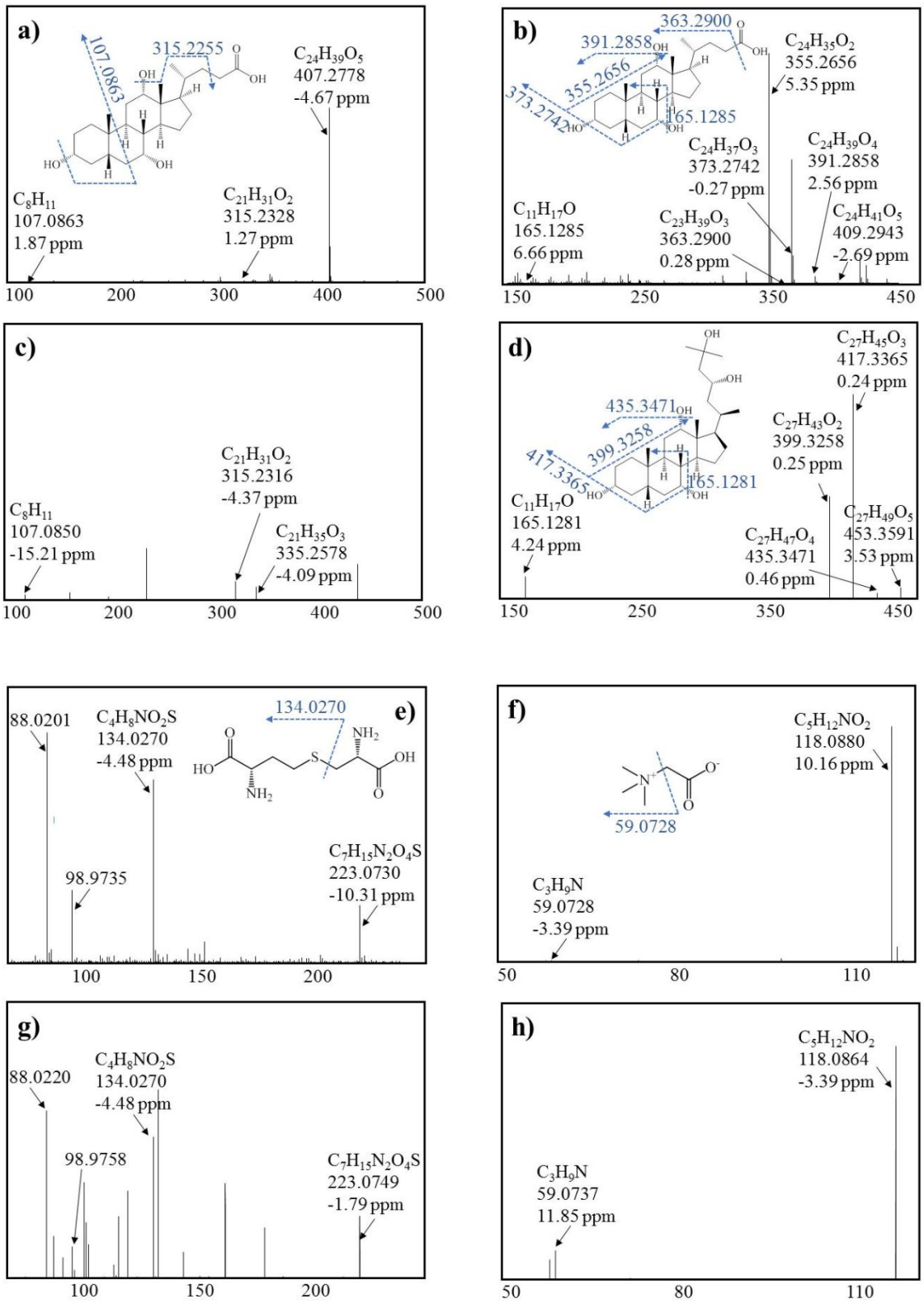

Figure S16. Mass spectra of standards of Cholate (a, ESI^- ion mode), Cholate (b, ESI^+ ion mode), L-Cystathionine (e), and Betaine (f). Mass spectra of Cholate (c, ESI^- ion mode), Cholestane-pentol (d), L-Cystathionine (g), and Betaine (h) detected in zebrafish embryo.

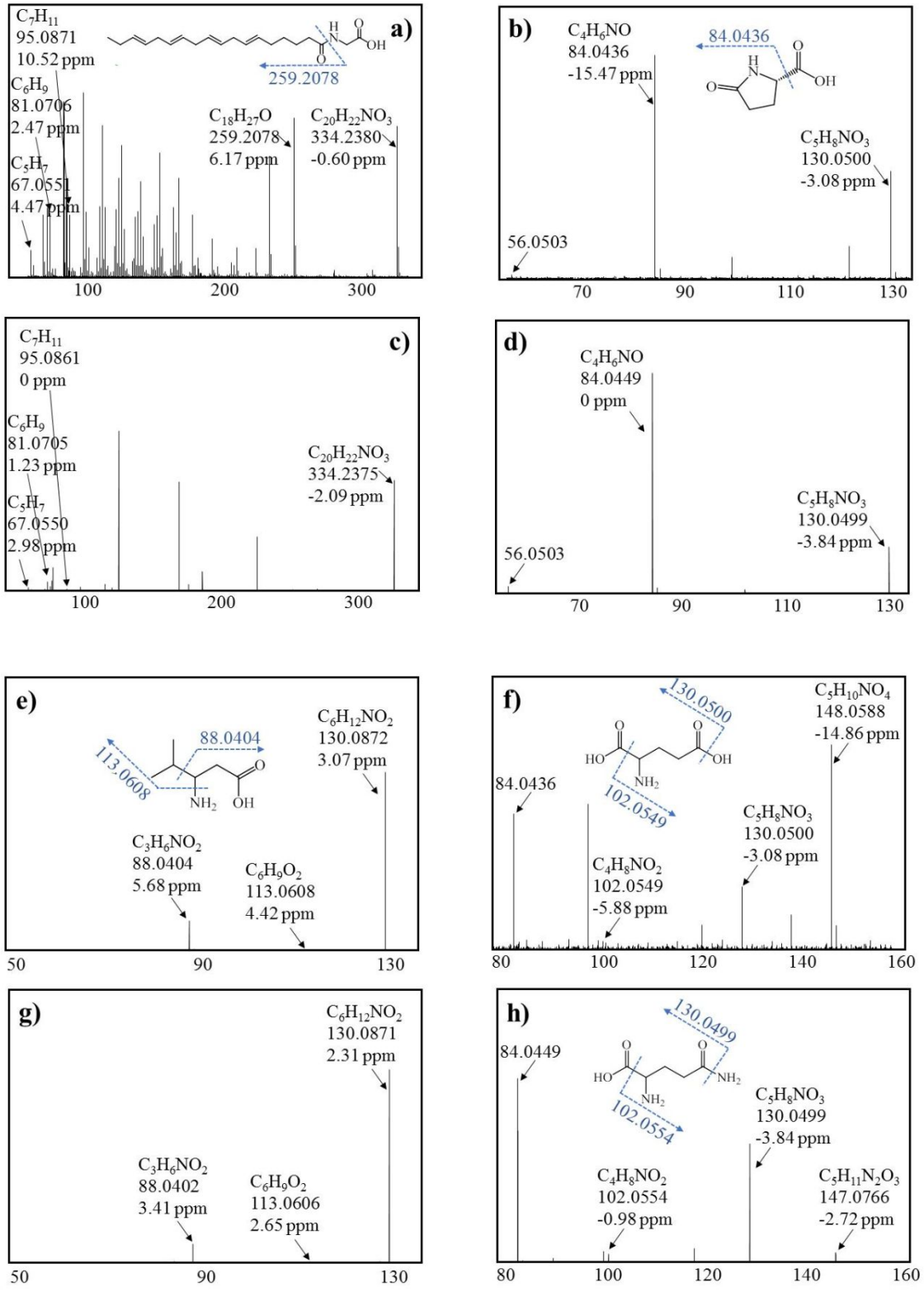

Figure S17. Mass spectra of standards of Stearidonoyl glycin (a), 5-Oxoproline (b), β-Leucine (e), and L-Glutamate (f). Mass spectra of Stearidonoyl glycin (c), 5-Oxoproline (d), β-Leucine (g), and L-Glutamine (h) detected in zebrafish embryo.

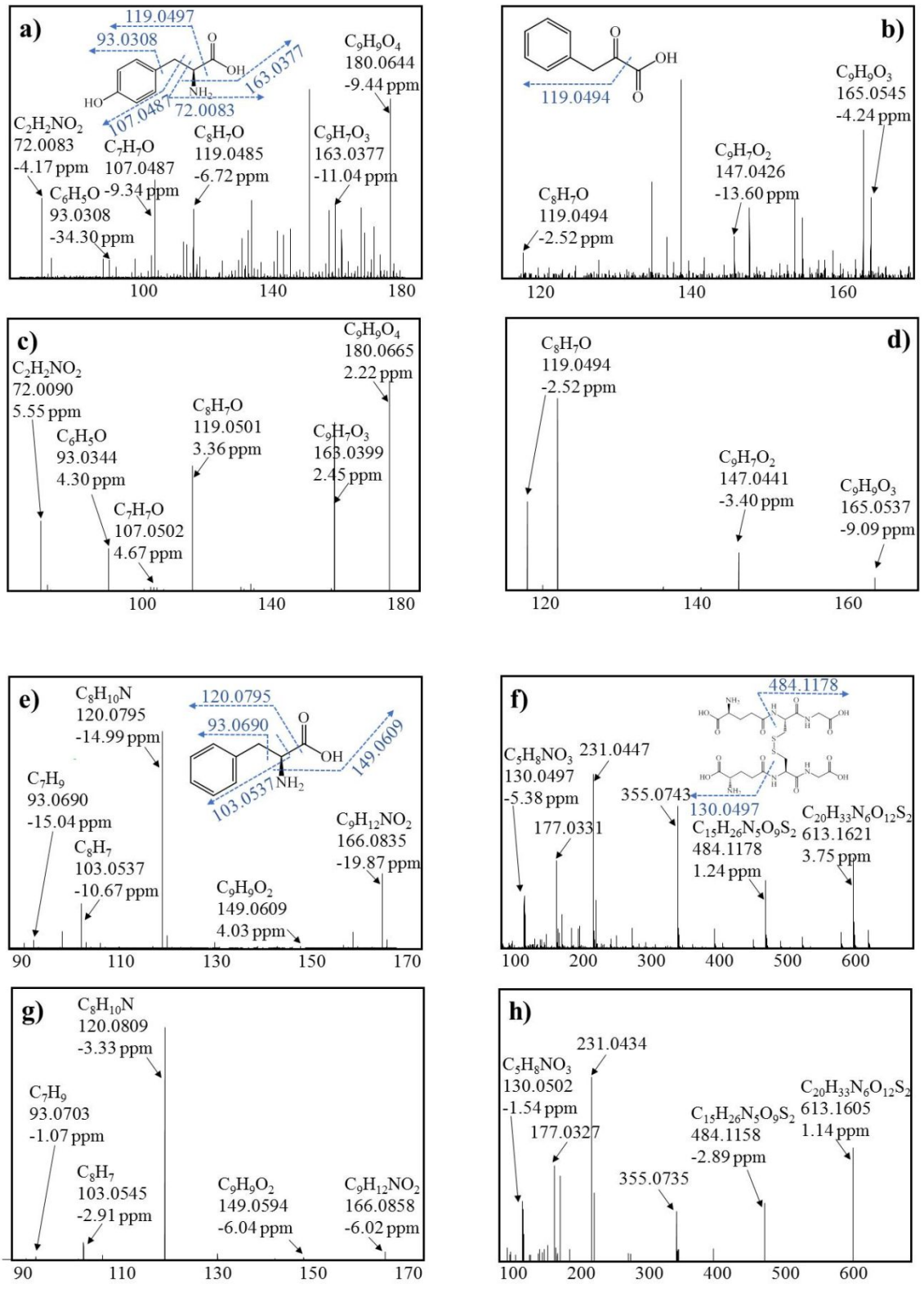

Figure S18. Mass spectra of standards of L-Tyrosine (a), Phenyl-pyruvate (b), Phenylalanine (e), and GSSG (f). Mass spectra of L-Tyrosine (c), Phenyl-pyruvate (d), Phenylalanine (g), and GSSG (h) detected in zebrafish embryo.

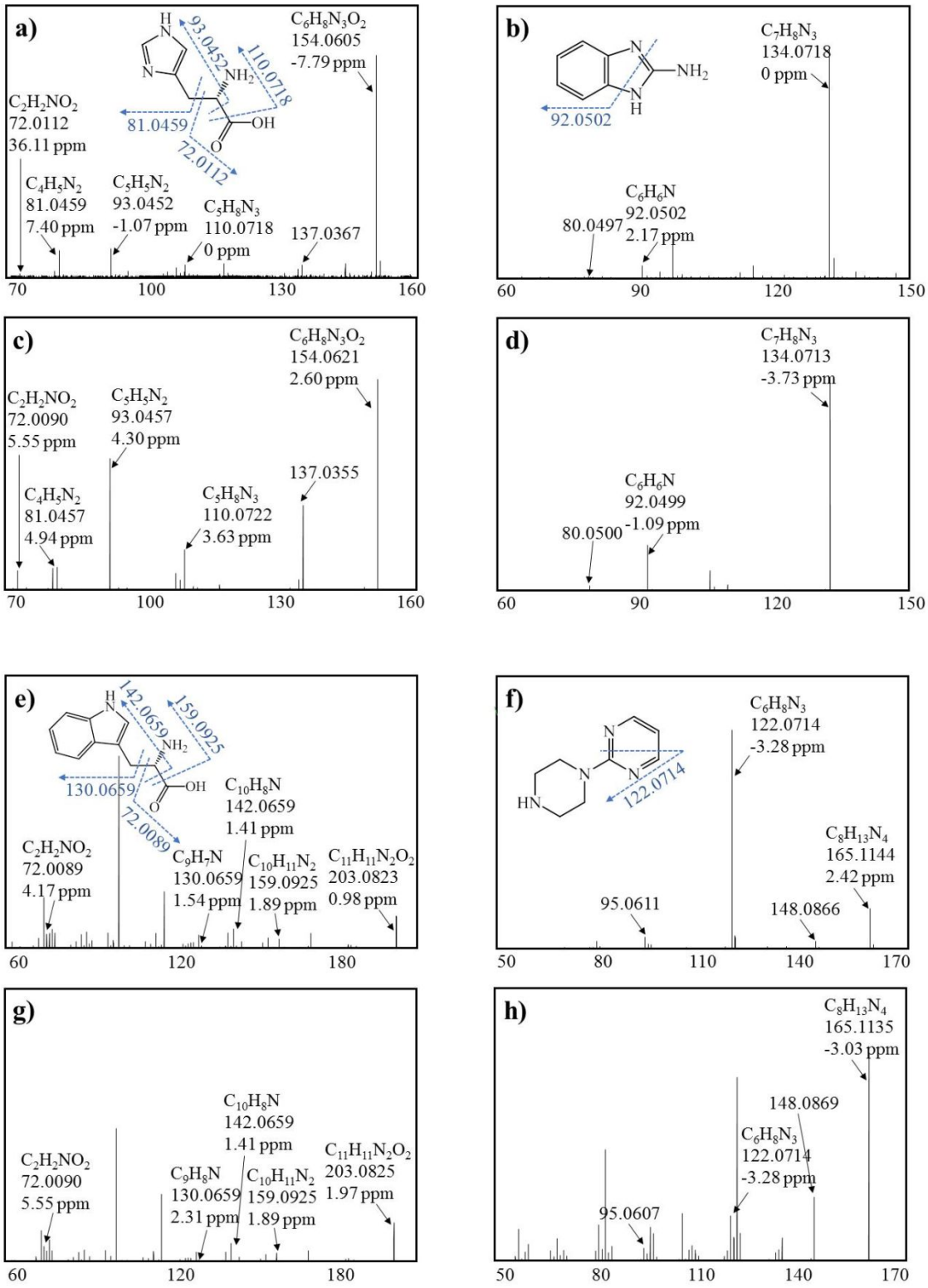

Figure S19. Mass spectra of standards of L-Histidine (a), 2-Aminobenzimidazole (b), L-Tryptophan (e), and 1-(2-Pyrimidyl)piperazine (f). Mass spectra of L-Histidine (c), 2-Aminobenzimidazole (d), L-Tryptophan (g), and 1-(2-Pyrimidyl)piperazine (h) detected in zebrafish embryo.

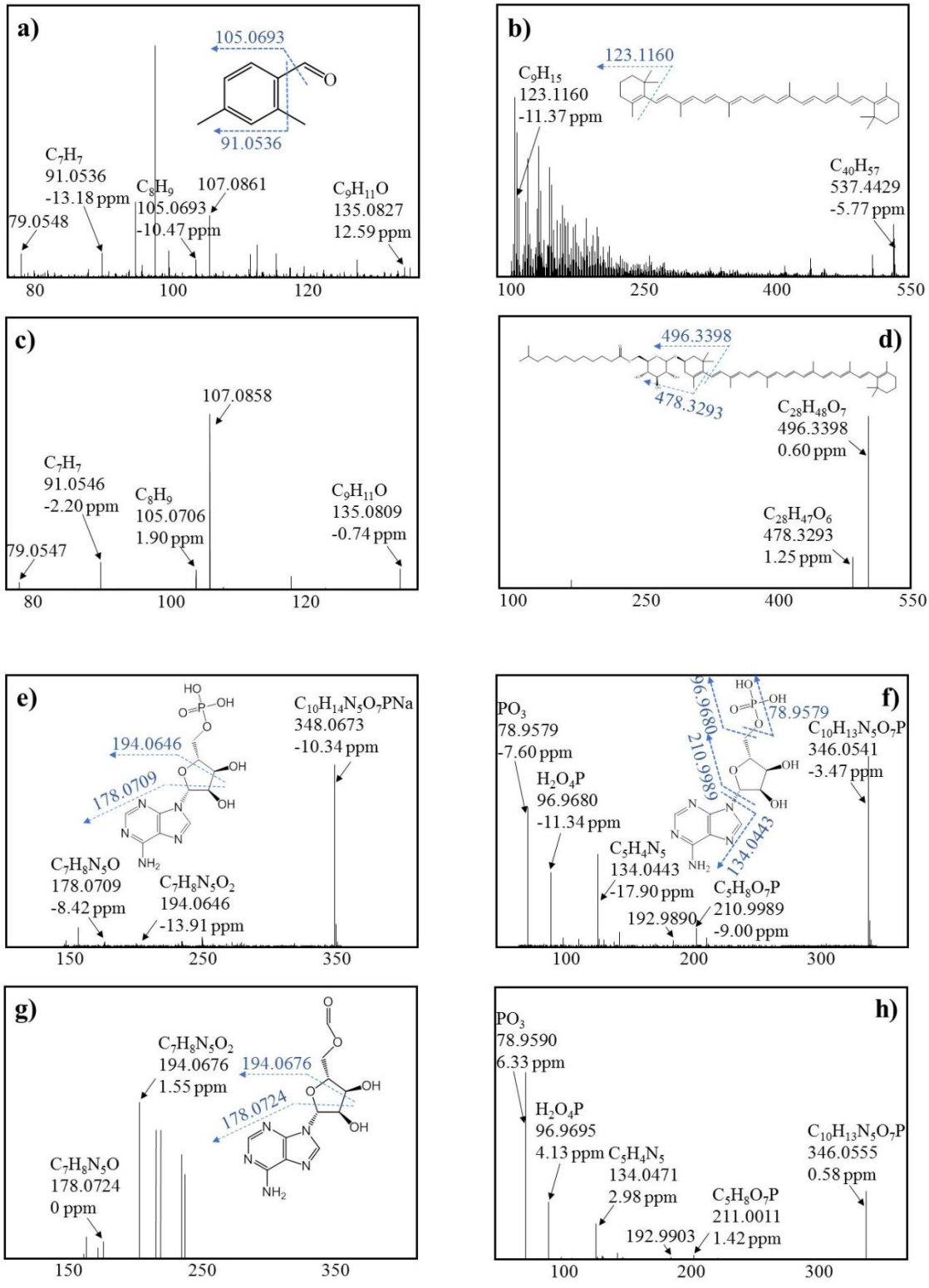

Figure S20. Mass spectra of standards of 2,4-Dimethylbenzaldehyde (a), β-Carotene (b), AMP (e, ESI^+ ion mode), and AMP (f, ESI^- ion mode). Mass spectra of 2,4-Dimethylbenzaldehyde (c), β-Carotene-Glucopyranoside (d), AMP analogue (g), and AMP (h, ESI^- ion mode) detected in zebrafish embryo.

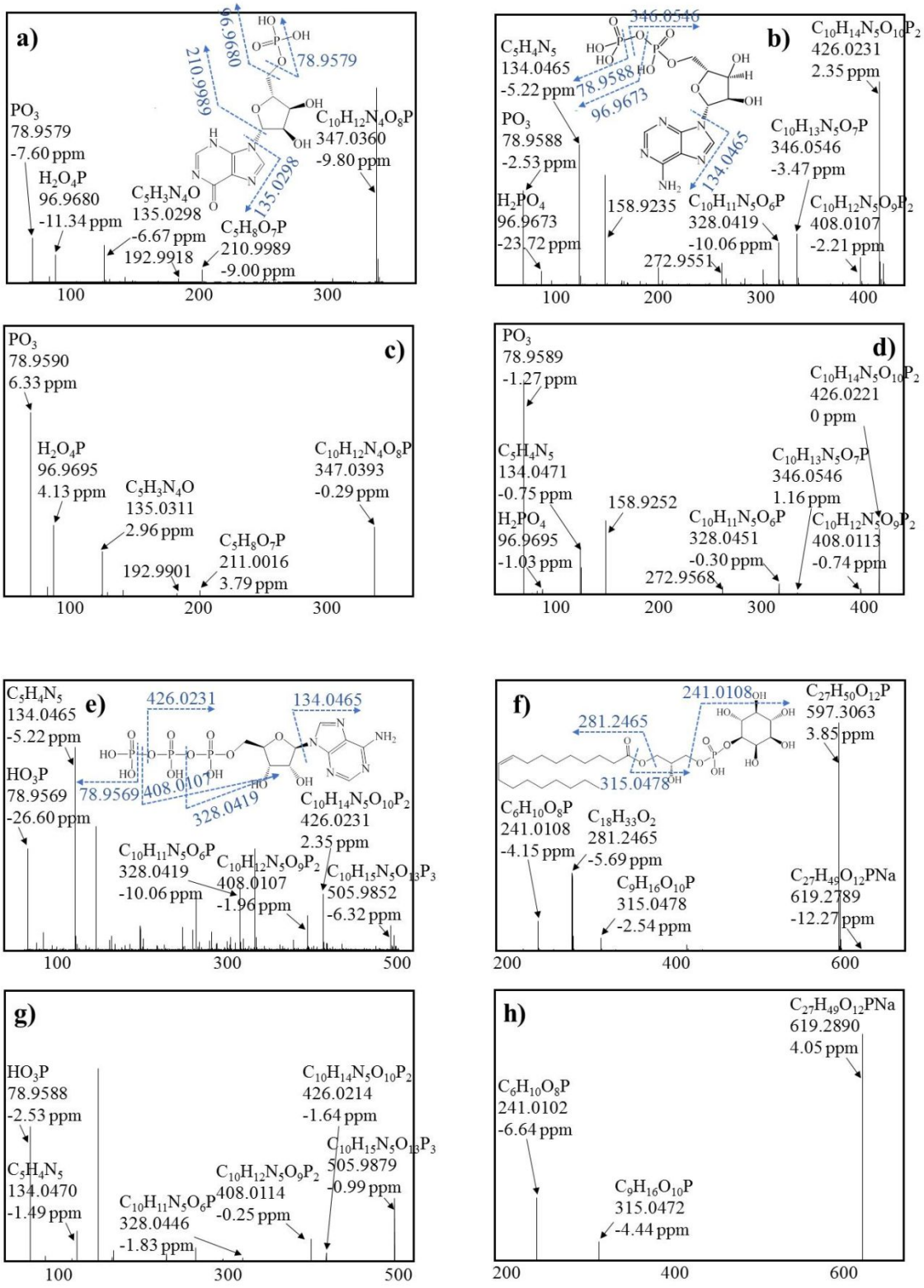

Figure S21. Mass spectra of standards of IMP (a), ADP (b), ATP (e), and LPI (f). Mass spectra of IMP (c), ADP (d), ATP (g), and LPI (h) detected in zebrafish embryo.

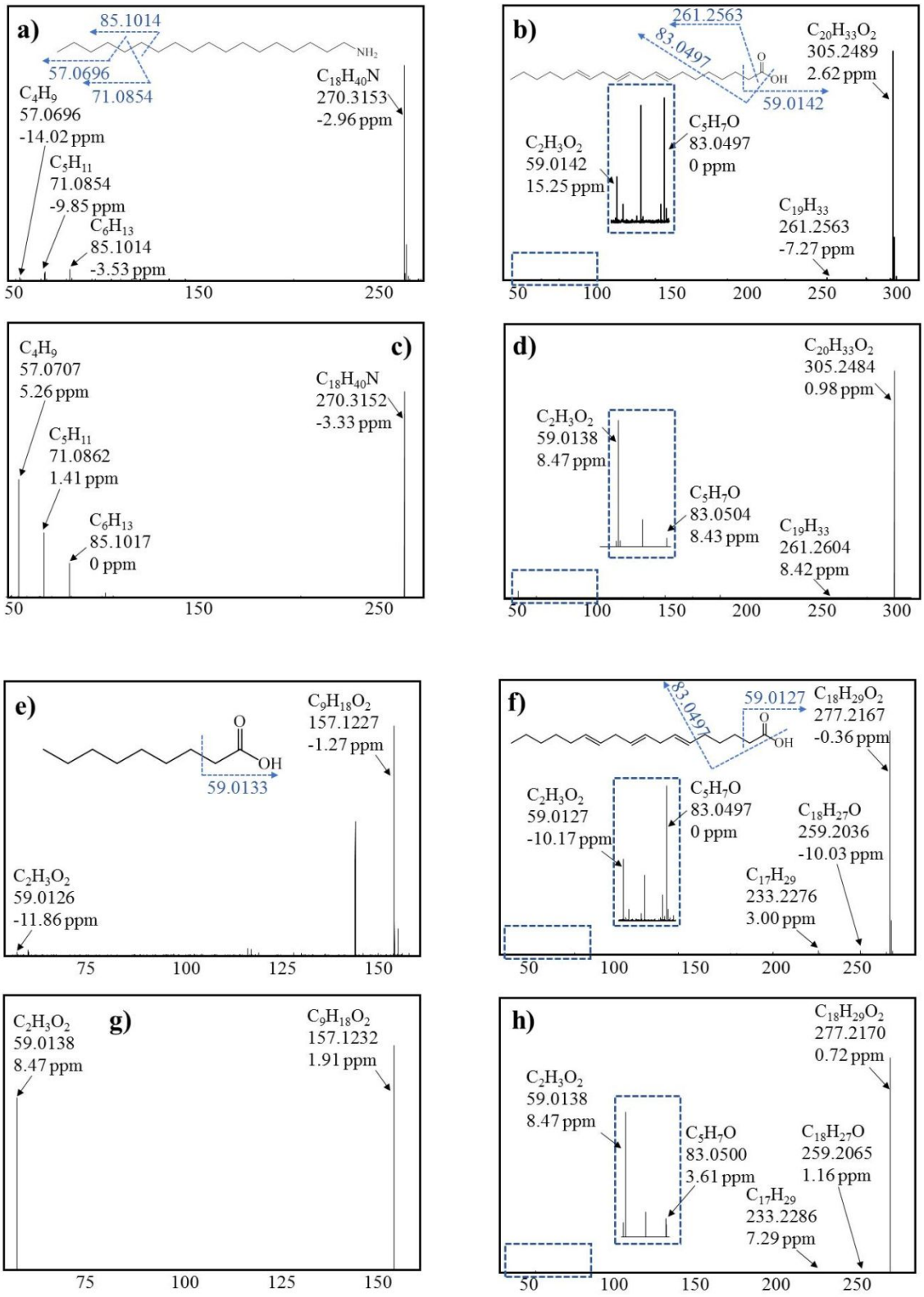

Figure S22. Mass spectra of standards of Octadecyl amine (a), Diho-γ-Lin (b), Nonanoic acid (e), and γ-Lin (f). Mass spectra of Octadecyl amine (c), Diho-γ-Lin (d), Nonanoic acid (g), and γ-Lin (h) detected in zebrafish embryo.

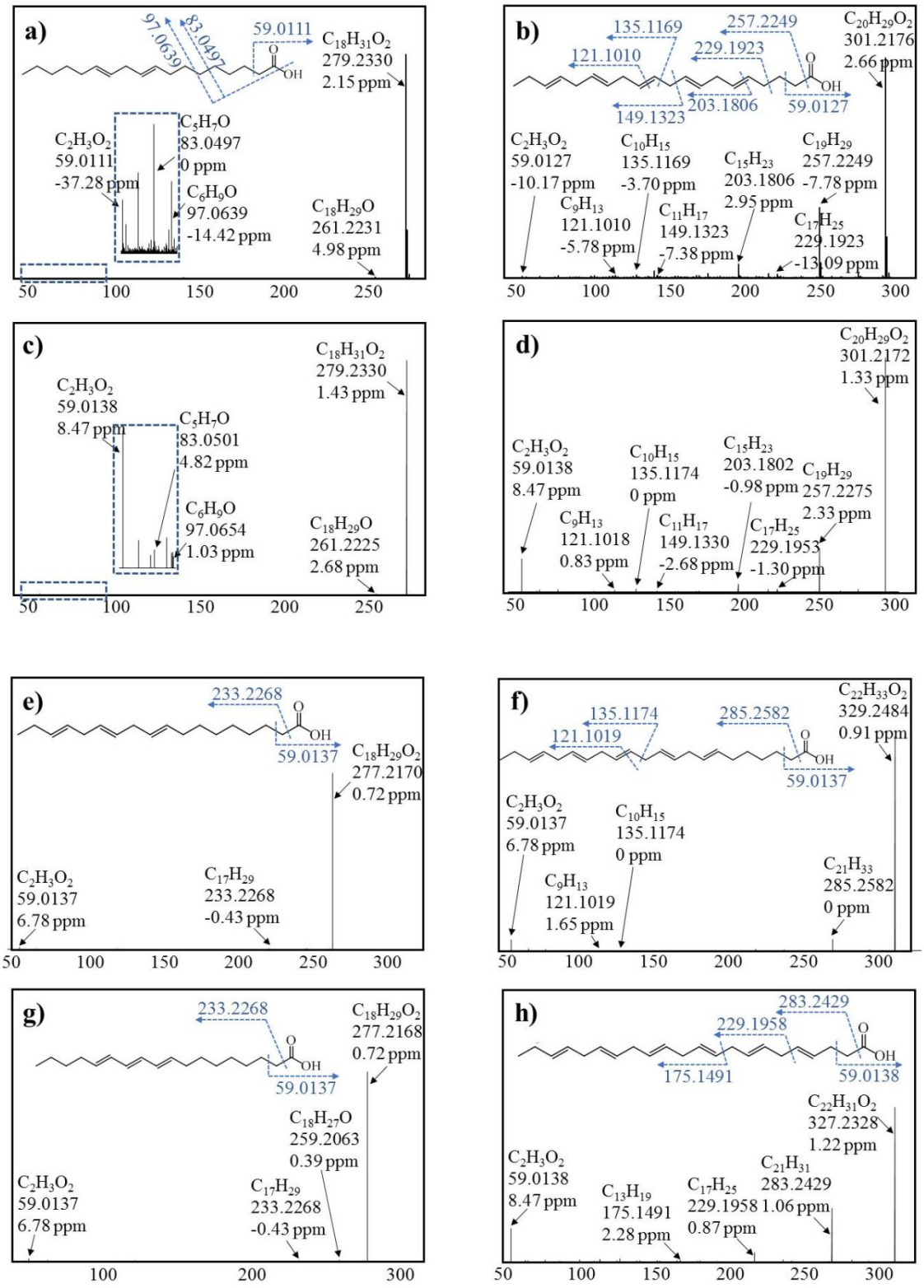

Figure S23. Mass spectra of standards of Lin (a), and EPA (b). Mass spectra of Lin (c), EPA (d), α-Lin (e), DPA (f), α-Eleostearic acid (g) and Docosahexaenoic acid (DHA), (h) detected in zebrafish embryo.

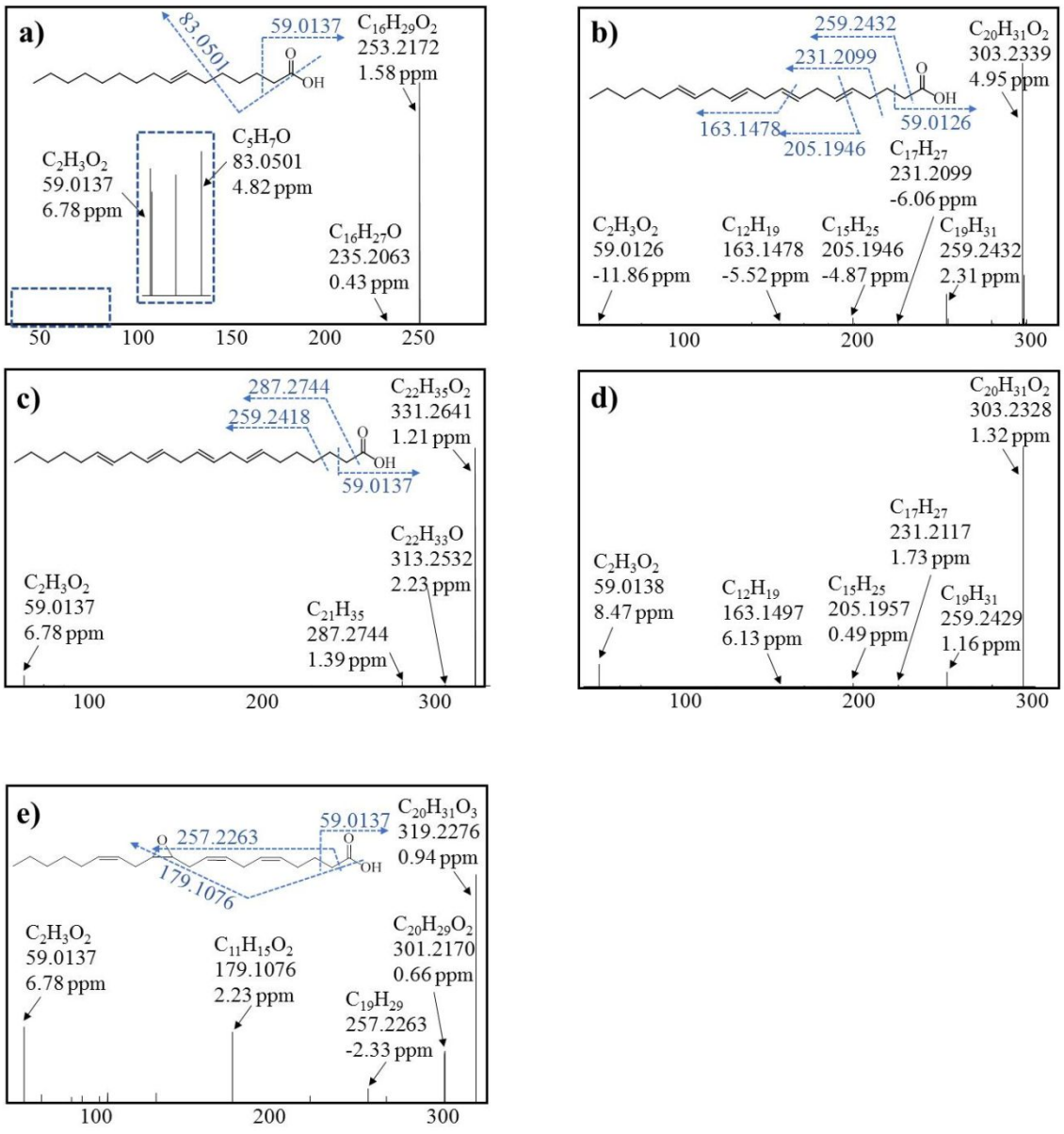

425

426 **Figure S24.** Mass spectra of standards of Ara (b). Mass spectra of Hexadecenoic acid (a),
427 Adrenic acid (c) Ara (d), and 11,12-EET (e) detected in zebrafish embryo.

428

429

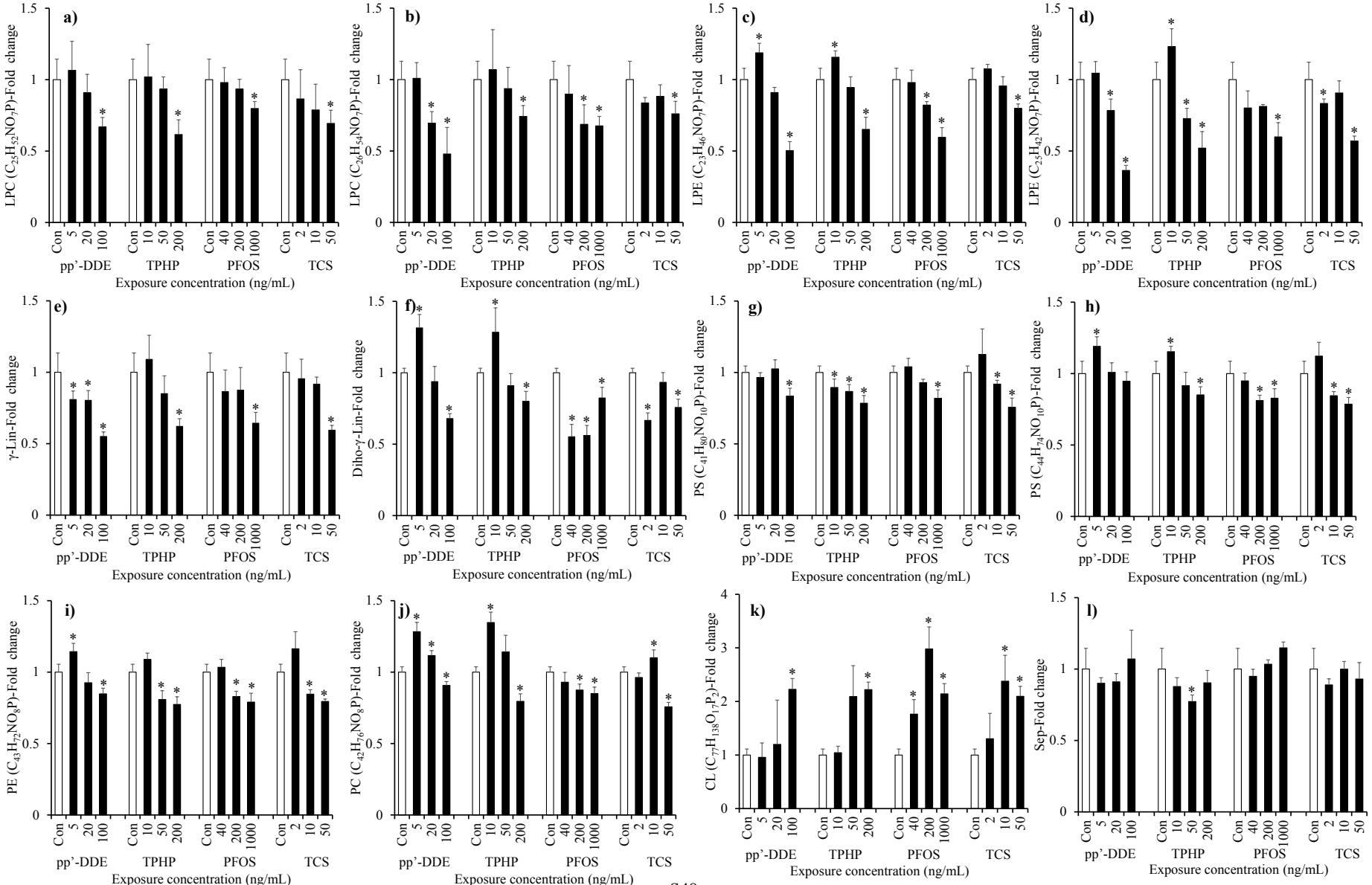
a)
LPC ($C_{25}H_{52}NO_7P$)-Fold change
b)
LPC ($C_{26}H_{54}NO_7P$)-Fold change
c)
LPE ($C_{23}H_{46}NO_7P$)-Fold change
d)
LPE ($C_{25}H_{42}NO_7P$)-Fold change
e)
γ-Lin-Fold change
f)
Diho-γ-Lin-Fold change
g)
PS ($C_{41}H_{80}NO_{10}P$)-Fold change
h)
PS ($C_{44}H_{74}NO_{10}P$)-Fold change
i)
PE ($C_{43}H_{72}NO_8P$)-Fold change
j)
PC ($C_{42}H_{76}NO_8P$)-Fold change
k)
CL ($C_{77}H_{138}O_{17}P_2$)-Fold change
l)
Sep-Fold change
Con 5 20 100
Con 10 50 200
Con 40 200 1000
Con 2 10 50
pp'-DDE
TPHP
PFOS
TCS
Exposure concentration (ng/mL)

Figure S25. Dose-response of LPCs (a-b), LPEs (c-d), linoleate related PUFAs (e-f), PLs (g-j), CL (k) and Sep (l) in zebrafish embryos after exposures to pp´-DDE, TPHP, PFOS, and TCS.

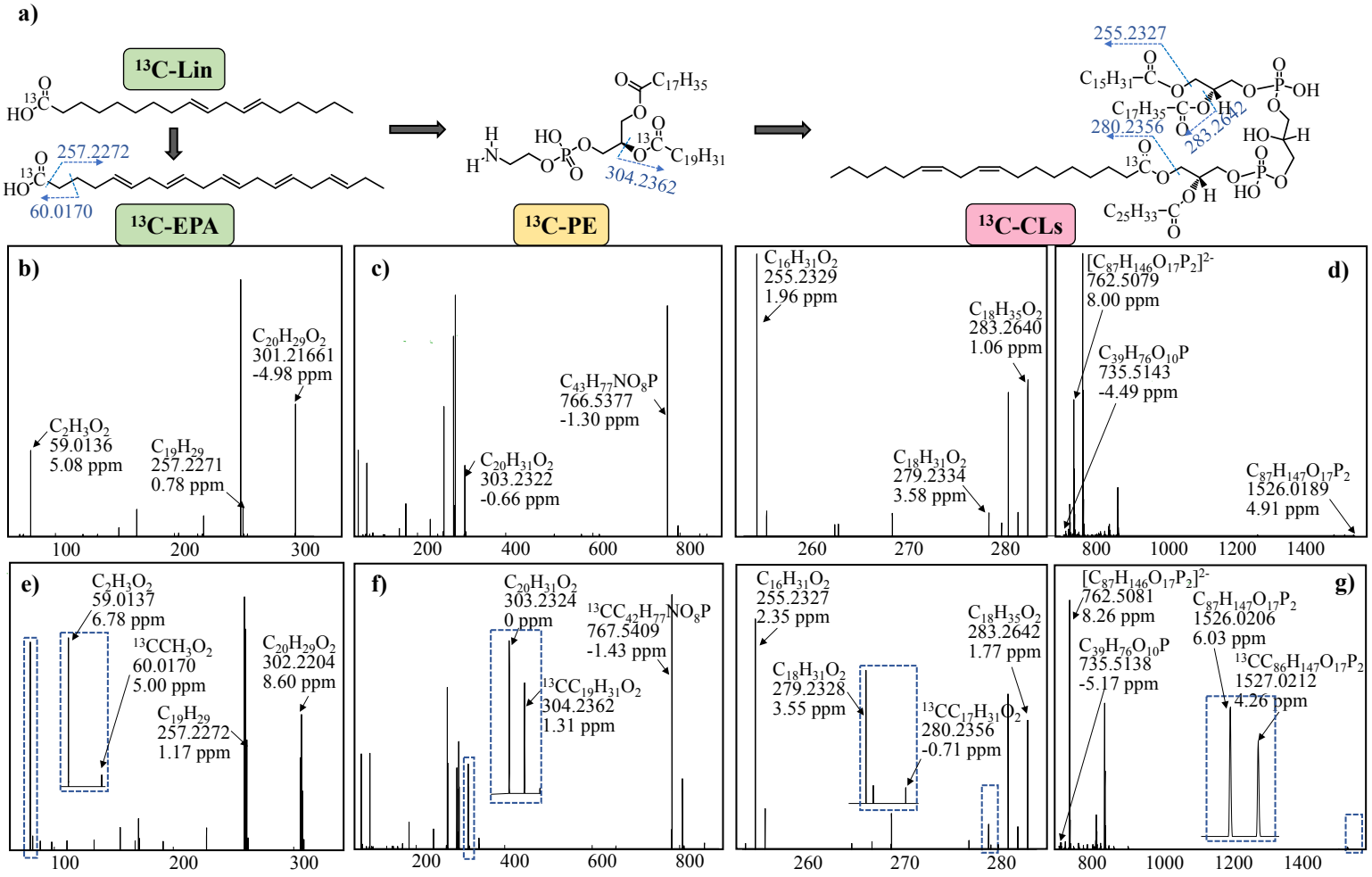

Figure S26. Metabolic pathways between CLs and linoleate related PUFAs. a) The detected ^{13}C-labelled metabolites and their metabolic relationships in zebrafish embryos exposed to ^{13}C-labeled linoleate. Mass spectra of endogenous EPA ($C_{20}H_{30}O_2$, b), PE ($C_{43}H_{78}NO_8P$, c), and CL ($C_{87}H_{148}O_{17}P_2$, d) in zebrafish embryos, and their corresponding ^{13}C-labeled compounds ($^{13}CC_{19}H_{30}O_2$, e; $^{13}CC_{42}H_{78}NO_8P$, f; $^{13}CC_{86}H_{148}O_{17}P_2$, g).

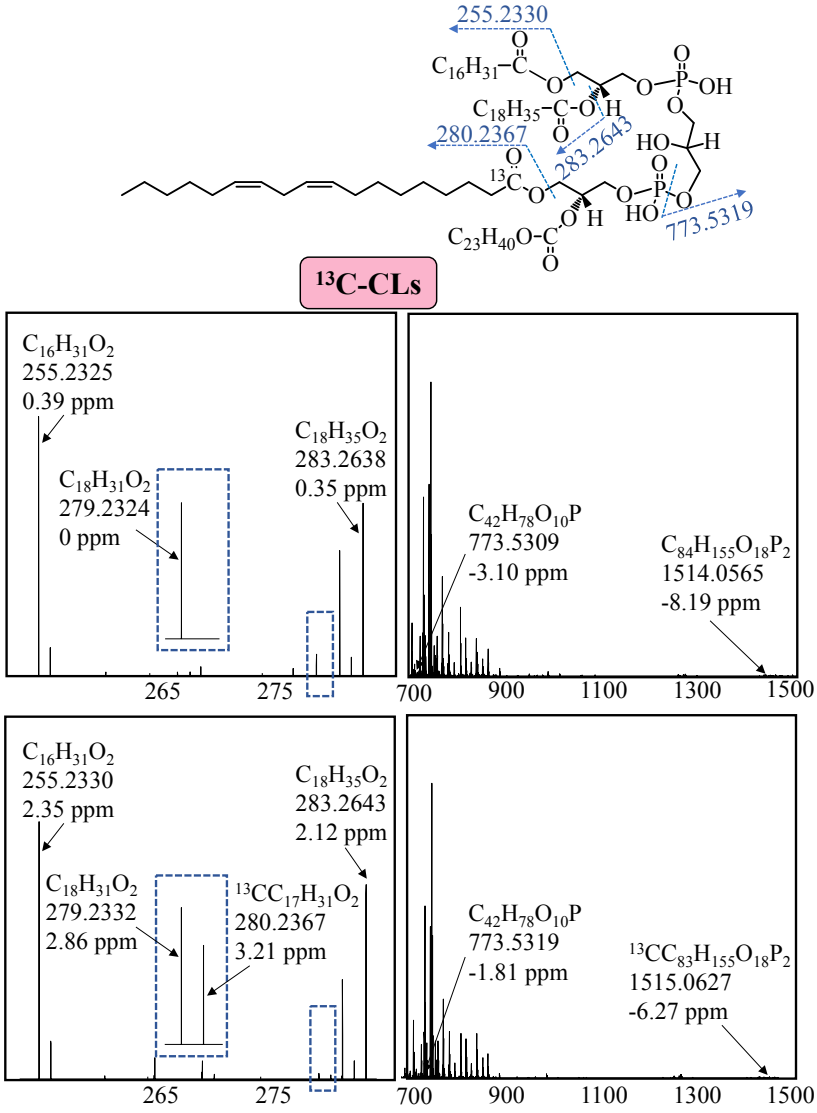

Figure S27. Mass spectra of endogenous CL ($C_{84}H_{156}O_{18}P_2$) in zebrafish embryos, and their corresponding ^{13}C-labeled compounds ($^{13}CC_{83}H_{156}O_{18}P_2$).

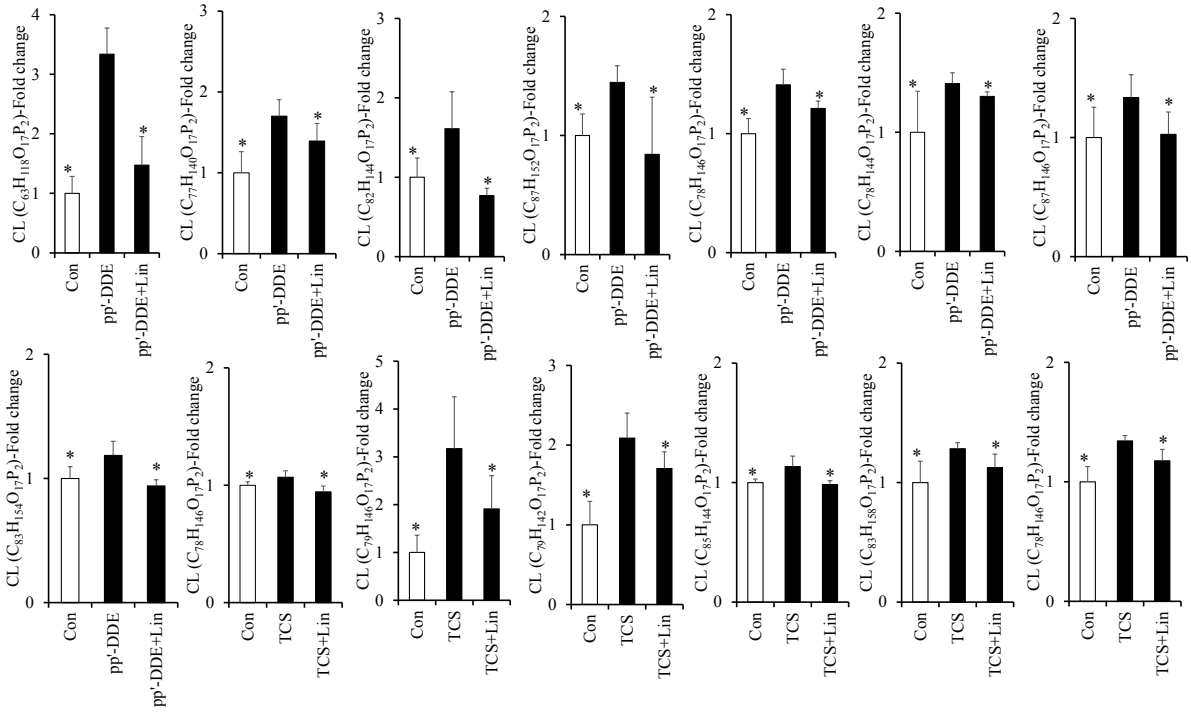

Figure S28. Variations in CL levels in zebrafish embryos exposed to individual chemicals (pp´-DDE or TCS) or co-exposed to chemicals and linoleate (pp´-DDE+ linoleate or TCS+ linoleate).

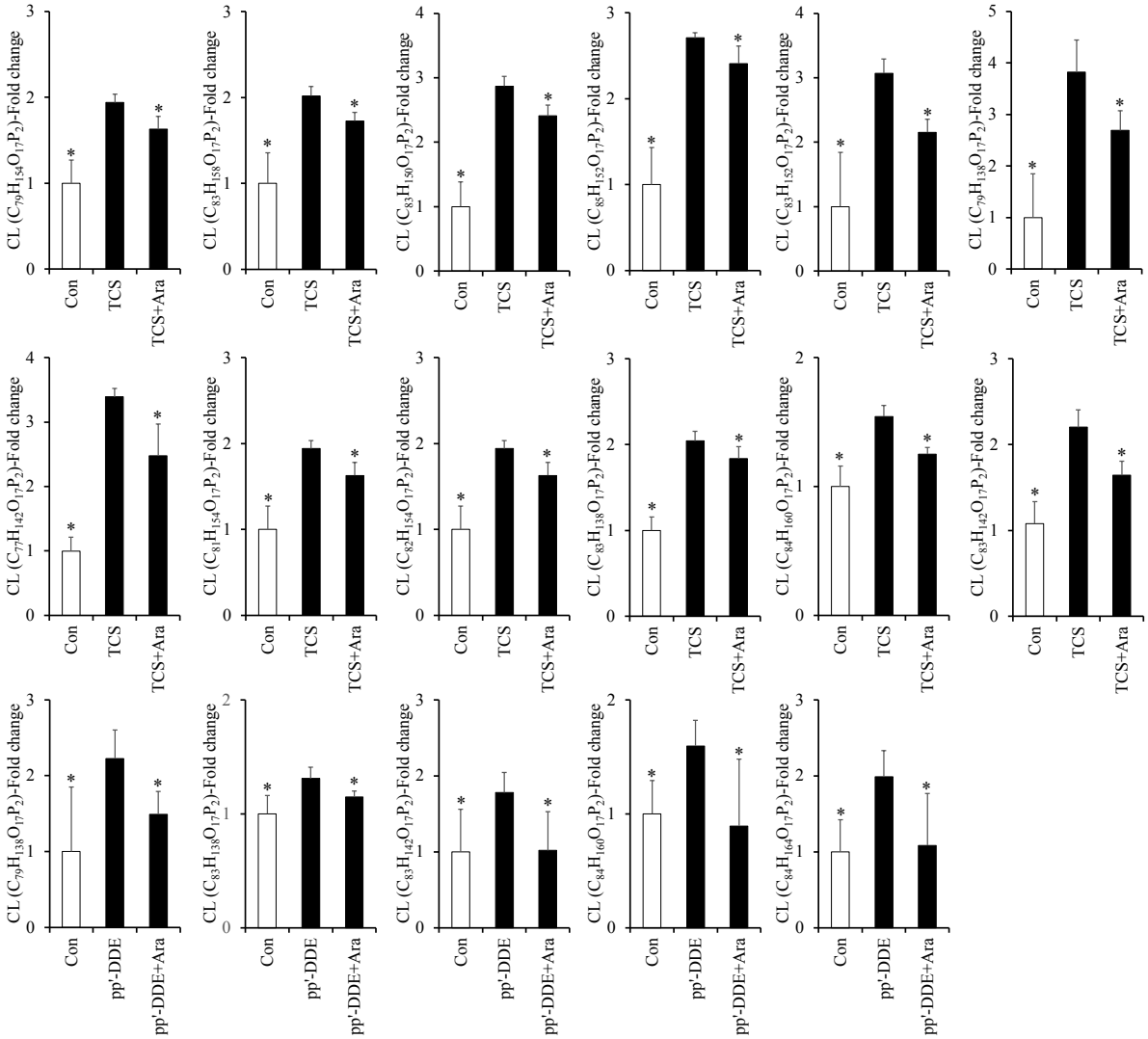

Figure S29. Variations in CL levels in zebrafish embryos exposed to individual chemicals (pp´-DDE or TCS) or co-exposed to chemicals and arachidonate (pp´-DDE+ arachidonate or TCS+ arachidonate).

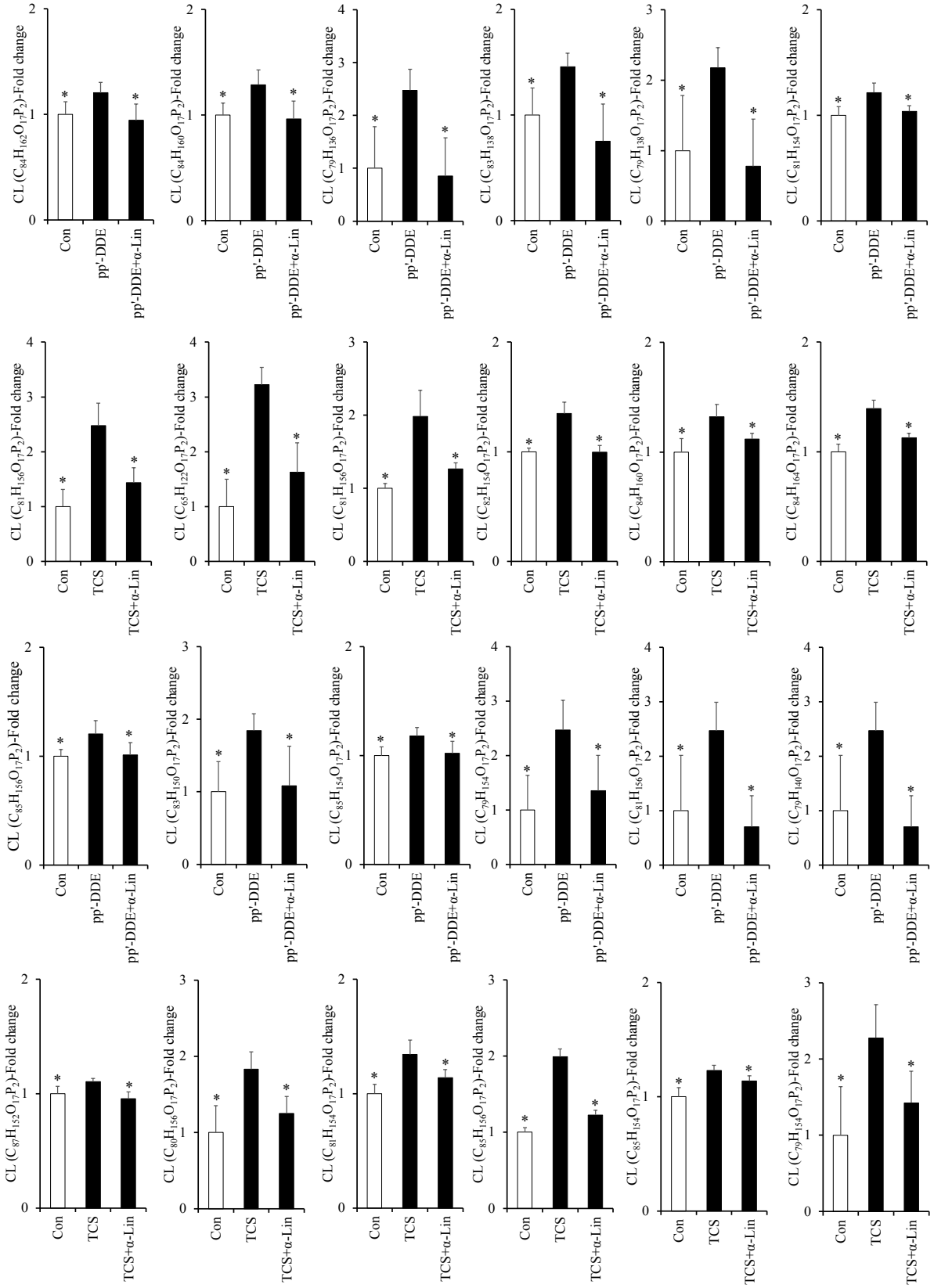

Figure S30. Variations in CL levels in zebrafish embryos exposed to individual chemicals (pp´-DDE or TCS) or co-exposed to chemicals and α-linoleate (pp´-DDE+α-linoleate or TCS+α-linoleate).

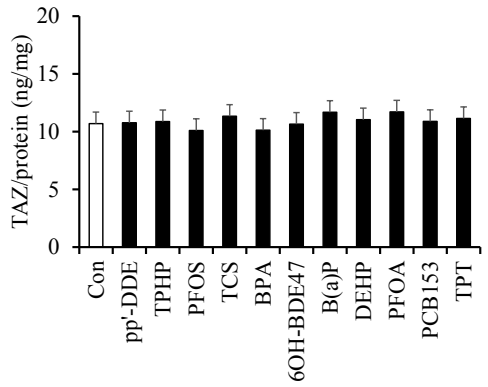

462

463 **Figure S31.** Levels of TAZ in zebrafish embryos exposed to the 11 chemicals.

464

465

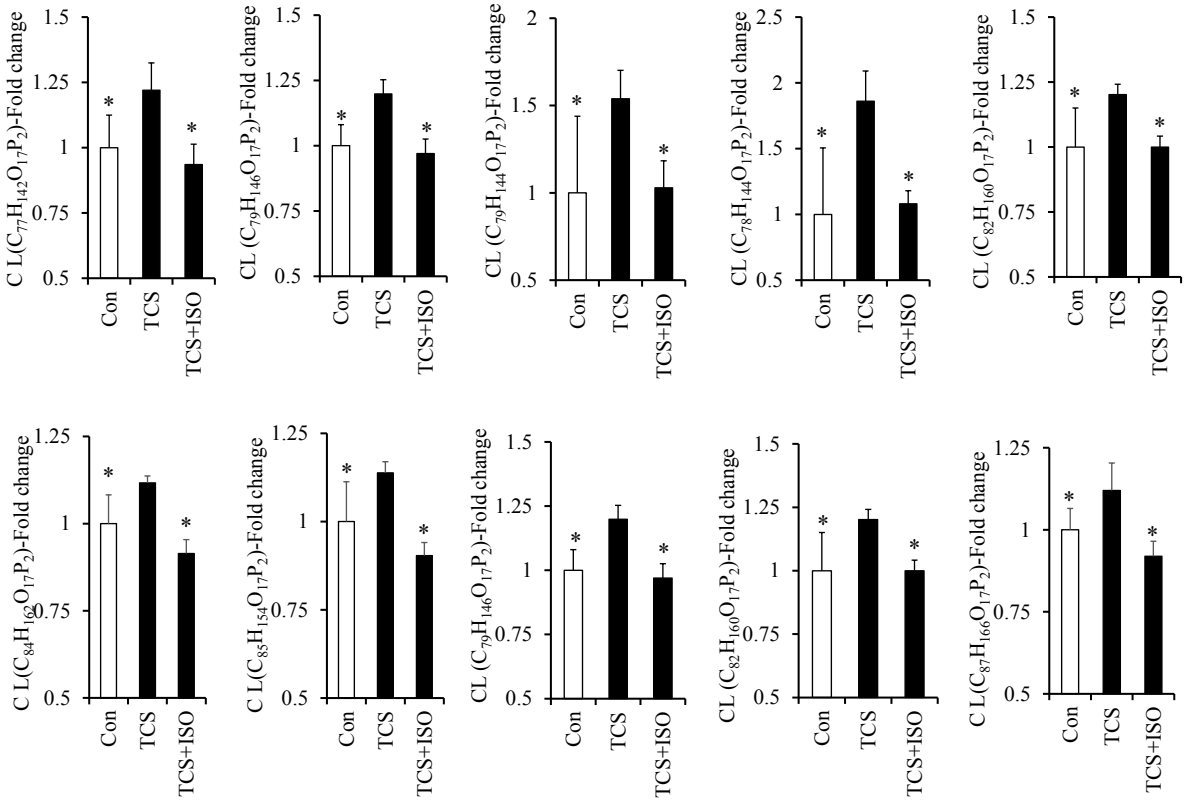

Figure S32. Variations in CL levels in zebrafish embryos exposed to TCS or co-exposed to TCS and ISO.

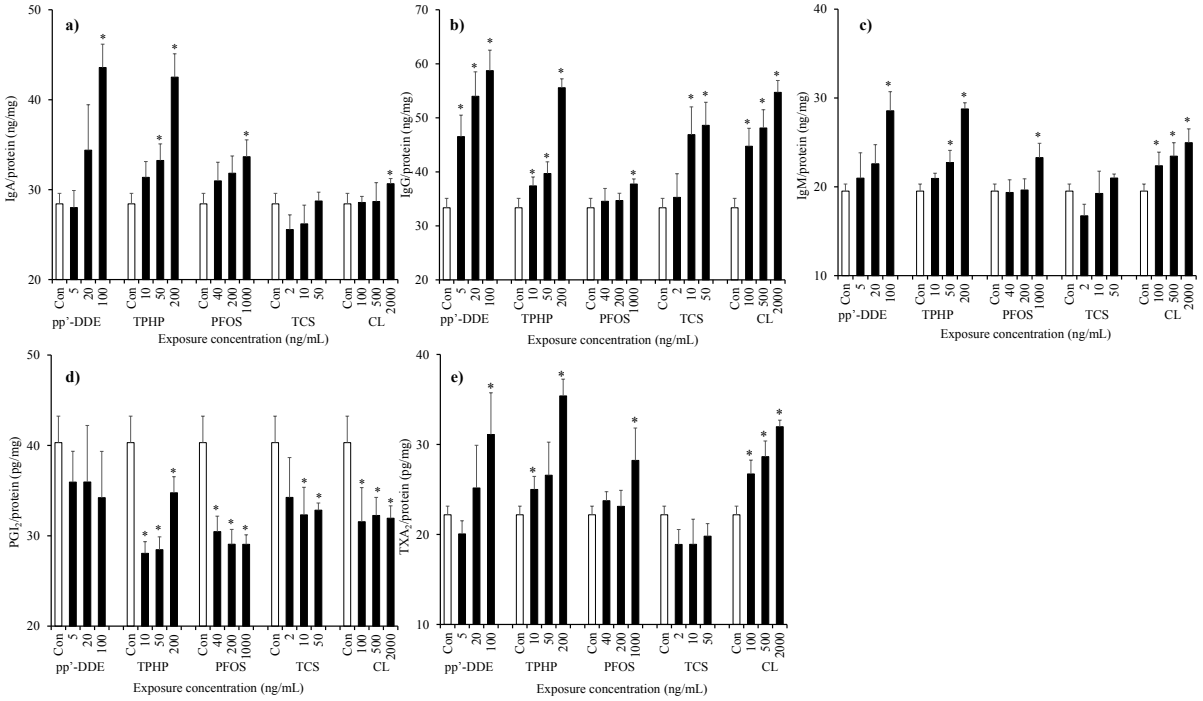

Figure S33. Levels of ACAs (a-c), PGI_2 (d), and TXA_2 (e) in zebrafish embryos exposed to the CL disrupting chemicals (pp´-DDE, TPHP, PFOS, and TCS) and CL at different concentrations.

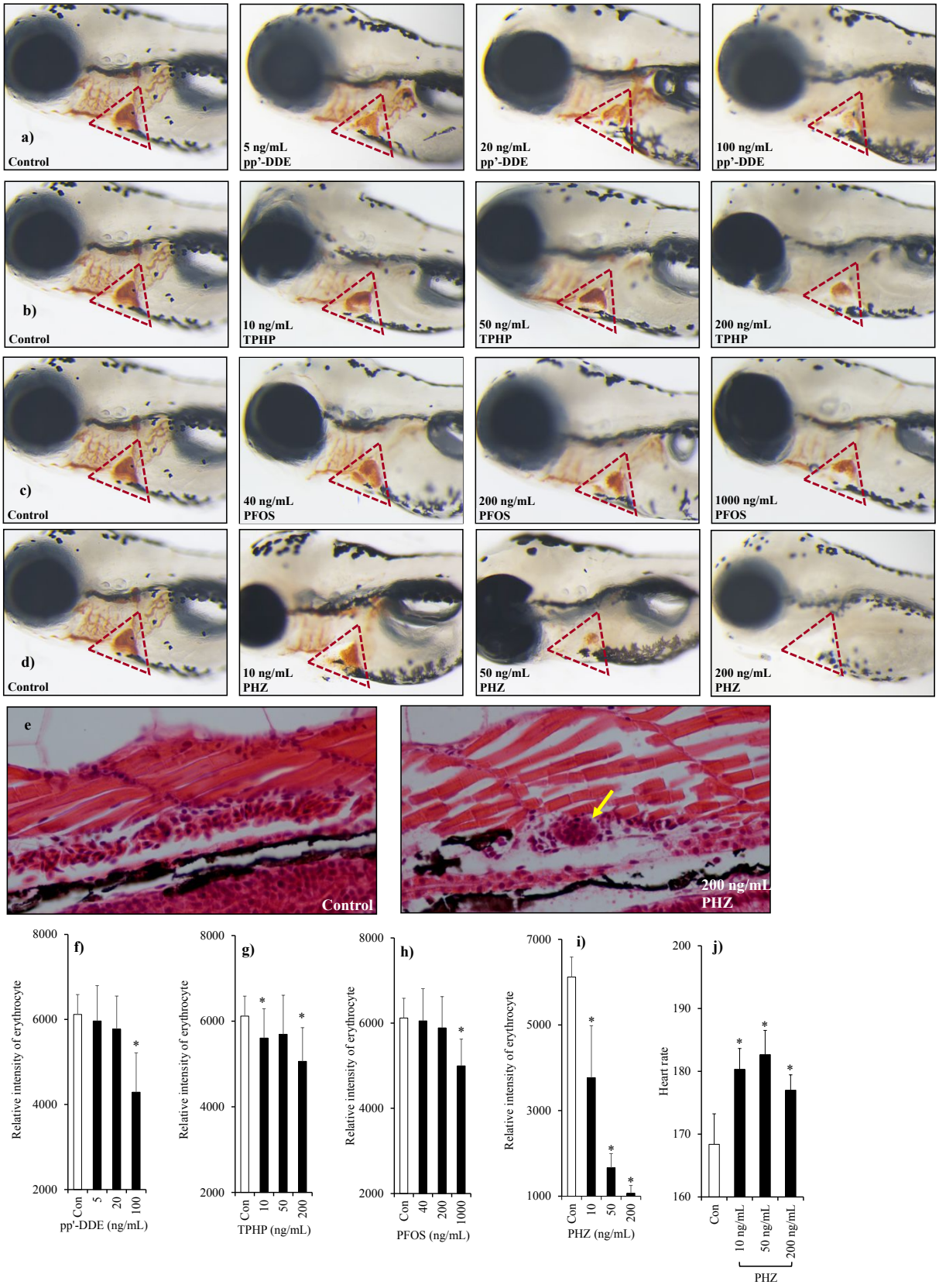

Figure S34. Metabolic disorders of CLs promote thrombosis. O-dianisidine staining of heart RBCs in zebrafish embryos exposed to pp´-DDE (a), TPHP (b), PFOS (c) and PHZ (d) at different concentrations. Histopathological examination of thrombus in blood vessels of zebrafish embryo exposed to PHZ (i). RBC intensities in response to exposure to pp´-DDE (f),

TPHP (g), PFOS (h) and PHZ (i) at different concentrations. (j) Heart rates in zebrafish embryos exposed to PHZ.

REFERENCES

1. Gao, S.; Wan, Y.; Li, W.; Huang, C. Visualized networking of co-regulated lipids in human blood based on high-throughput screening data: implications for exposure assessment. *Environ. Sci. Technol.* **2019**, *53*, 2862-2872.
2. Koeberlin, M. S.; Snijder, B.; Heinz, L. X.; Baumann, C. L.; Fauster, A.; Vladimer, G. I.; Gavin, A. C.; Superti-Furga, G. A conserved circular network of coregulated lipids modulates innate immune responses. *Cell* **2015**, *162*, 170-183.
3. Kind, T.; Tsugawa, H.; Cajka, T.; Ma, Y.; Lai, Z.; Mehta, S. S.; Wohlgemuth, G.; Barupal, D. K.; Showalter, M. R.; Arita, M.; Fiehn, O. Identification of small molecules using accurate mass MS/MS search. *Mass. Spectrom. Rev.* **2018**, *37*, 513-532.
4. Caspi, R.; Altman, T.; Billington, R.; Dreher, K.; Foerester, H.; Fulcher, C. A.; Holland, T. A.; Keseler, I. M.; Kothari, A.; Kubo, A.; Krummenacker, M.; Latendresse, M.; Mueller, L. A.; Ong, Q.; Paley, S.; Subhraveti, P.; Weaver, D. S.; Weerasinghe, D.; Zhang, P.; Karp, P. D. The MetaCyc database of metabolic pathways and enzymes and the BioCyc collection of pathway/genome databases. *Nucleic Acids Res.* **2016**, *44*, D471-D480.
5. Alex, F.; Craig, K.; Emilia, L.; Timothy, J.; Vivian, L.; Hau, D. D.; Liu, P.; Gautam, B.; Ly, S.; Guo, A. C.; Xia, J.; Liang, Y.; Shrivastava, S.; Wishart, D. S. SMPDB: the small molecule pathway database. *Nucleic Acids Res.* **2010**, *38*, D480-D487.
6. Hu, W.; Jia, Y.; Kang, Q.; Peng, H.; Ma, H.; Zhang, S.; Hiromori, Y.; Kimura, T.; Nakanishi, T.; Zheng, L.; Qiu, Y.; Zhang, Z.; Wan, Y.; Hu, J. Screening of house dust from Chinese homes for chemicals with liver x receptors binding activities and characterization of atherosclerotic activity using an in vitro macrophage cell line and ApoE$^{-/-}$ mice. *Environ. Health. Persp.* (https://doi.org/10.1289/EHP5039)
7. Schymanski, E. L.; Jeon, J.; Gulde, R.; Fenner, K.; Ruff, M.; Singer, H. P.; Hollender, J. Identifying small molecules via high resolution mass spectrometry: communicating confidence. *Environ. Sci. Technol.* **2014**, *48*, 2097−2098.
8. Zheng, G.; Wan, Y.; Hu, J. Intrinsic clearance of xenobiotic chemicals by liver microsomes: assessment of trophic magnification potentials. *Environ. Sci. Technol.* **2016**, *50* 6343-6353.
9. Ashrap, P.; Zheng, G.; Wan, Y.; Li, T.; Hu, W.; Li, W.; Zhang, H.; Zhang, Z.; Hu, J. Discovery of a widespread metabolic pathway within and among phenolic xenobiotics. *Proc. Natl. Acad. Sci. USA* **2017**, *114*, 6062-6067.
10. Kang, Q.; Gao, F.; Zhang, X.; Wang, L.; Hu, J. Nontargeted identification of per- and polyfluoroalkyl substances in human follicular fluid and their blood-follicle transfer. *Environ. Int.* **2020**, *139*, 105686.
11. Varlet-Marie, E.; Ashenden, M. J.; Moerkeberg, J.; Vela, C.; Audran, M. Relevance of di(2-ethylhexyl)phthalate blood levels for blood transfusion detection. *Bioanalysis* **2014**, *6*, 1591-1595.
12. Zhao, F.; Chen, M.; Gao, F.; Shen, H.; Hu, J. Organophosphorus flame retardants in

pregnant women and their transfer to chorionic villi. *Environ. Sci. Technol.* **2017**, *51*, 6489-6497.

13. Escarrone, A. L. V.; Caldas, S. S.; Soares, B. M.; Martins, S. E.; Primel, E. G.; Nery, L. E. M. A vortex-assisted mspd method for triclosan extraction from fish tissues with determination by LC-MS/MS. *Anal Methods-UK.* **2014**, *6*, 8306-8313.
14. Notarnicola, M.; Misciagna, G.; Tutino, V.; Chiloiro, M.; Osella, A. R.; Guerra, V.; Bonfiglio, C.; Caruso, M. G. Increased serum levels of lipogenic enzymes in patients with severe liver steatosis. *Lipids. Health. Dis.* **2012**, *11*, 145.
15. Cavalier, J.; Ransac, S.; Verger, R.; Buono, G. Inhibition of human gastric and pancreatic lipases by chiral alkylphosphonates. a kinetic study with 1,2-didecanoyl-sn-glycerol monolayer. *Chem. Phys. Lipids.* **1999**, *100*, 3-31.
16. Mortaud, S.; Donsez-Darcel, E.; Roubertoux, P. L.; Degrelle, H. Murine steroid sulfatase (MSTS): purification, characterization and measurement by ELISA. *J. Steroid Biochem.* **1995**, *52*, 91-96.
17. Cuendet, M.; Mesecar, A. D.; Dewitt, D. L.; Pezzuto, J. M. An ELISA method to measure inhibition of the COX enzymes. *Nat. Protoc.* **2006**, *1*, 1915-21.
18. Zaragoza-García1, O.; Guzmán-Guzmán, I. P.; Moreno-Godínez, M. E.; Navarro-Zarza, J. E.; Antonio-Vejar, V.; Ramírez, M.; Parra-Rojas, I. PON-1 haplotype (-108C>T, L55M, and Q192R) modulates the serum levels and activity PONase romoting an atherogenic lipid profile in rheumatoid arthritis patients. *Clin. Rheumatol.* **2020**, DOI: 10.1007/s10067-020-05218-w.
19. Dennis, E. A.; Cao, J.; Hsu, Y. H.; Magrioti, V.; Kokotos, G. Phospholipase A_2 enzymes: physical structure, biological function, disease implication, chemical inhibition, and therapeutic intervention. *Chem. Rev.* **2011**, *111*, 6130-6185.
20. Ren, M. D.; Phoon, C. K.; Schlame, M. Metabolism and function of mitochondrial cardiolipin. *Prog. Lipid Res.* **2014**, *55*, 1-16.
21. Zhao, Y.; Chen, Y. Q.; Li, S. Y.; Konrad, R. J.; Cao, G. Q. The microsomal cardiolipin remodeling enzyme acyl-CoA lysocardiolipin acyltransferase is an acyltransferase of multiple anionic lysophospholipids. *J. Lipid Res.* **2009**, *50*, 945-956.
22. Astudillo, A. M.; Balboa, M. A.; Balsinde, J. Selectivity of phospholipid hydrolysis by phospholipase A_2, enzymes in activated cells leading to polyunsaturated fatty acid mobilization. *BBA-Mol. Cell. Biol. L.* **2018**, *1864*, 772-783.
23. Meroni, P. L.; Borghi, M. O.; Raschi, E.; Tedesco, F. Pathogenesis of antiphospholipid syndrome: understanding the antibodies. *Nat. Rev. Rheumatol.* **2011**, *7*, 330-339.
24. Garcia, D.; Erkan, D. Diagnosis and management of the antiphospholipid syndrome. *New Engl J. Med.* **2018**, *378*, 2010-2021.
25. Cheng, Y.; Austin, S. C.; Rocca, B.; Koller, B. H.; Coffman, T. M.; Grosser, T.; Lawson, J. A.; FitzGerald, G. A. Role of prostacyclin in the cardiovascular response to thromboxane A_2. *Science* **2002**, *296*, 539-541.

559 26. Liu, H.; Chu, T.; Chen, L.; Gui, W.; Zhu, G. In vivo cardiovascular toxicity induced by
560 acetochlor in zebrafish larvae. *Chemosphere* **2017**, *181*, 600-608.
561 27. Zhu, X.; Liu, H.; Guo, S.; Xia, B.; Song, R.; Lao, Q.; Xuan, Y.; Li, C. A zebrafish
562 thrombosis model for assessing antithrombotic drugs. *Zebrafish* **2016**, *13*, 335-344.
563